How to Use Borehole Nuclear Magnetic Resonance

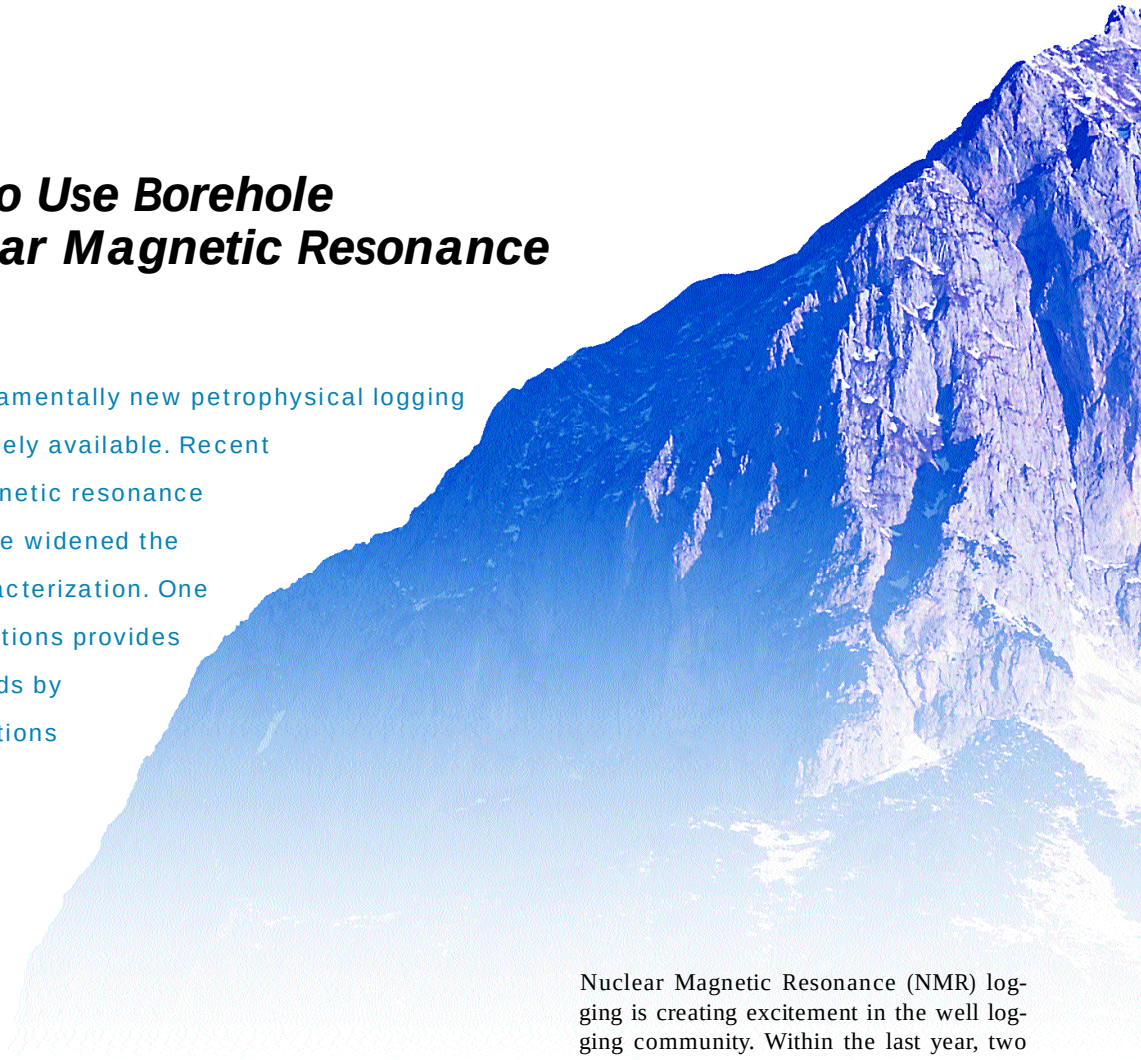

It is a rare event when a fundamentally new petrophysical logging measurement becomes routinely available. Recent developments in nuclear magnetic resonance measurement technology have widened the scope of formation fluid characterization. One of the most significant innovations provides new insight into reservoir fluids by partitioning porosity into fractions classed by mobility.

David Allen
Steve Crary
Bob Freedman
Sugar Land, Texas, USA

Marc Andreani
Werner Klopf
Milan, Italy

Rob Badry
Calgary, Alberta, Canada

Charles Flaum
Bill Kenyon
Robert Kleinberg
Ridgefield, Connecticut, USA

Patrizio Gossenberg
Agip S.p.A.
Milan, Italy

Jack Horkowitz
Dale Logan
Midland, Texas, USA

Julian Singer
Caracas, Venezuela

Jim White
Aberdeen, Scotland

For help in preparation of this article, thanks to Greg Gubelin, Schlumberger Wireline & Testing, Sugar Land, Texas, USA; Michael Herron, Schlumberger-Doll Research, Ridgefield, Connecticut, USA; James J. Howard, Phillips Petroleum Research, Bartlesville, Oklahoma, USA; Jack LaVigne, Schlumberger Wireline & Testing, Houston, Texas; Stuart Murchie and Kambiz A. Safinya, Schlumberger Wireline & Testing, Montrouge, France; Carlos E. Ollier, Schlumberger Wireline & Testing, Buenos Aires, Argentina; and Gordon Pirie, Consultation Services, Inc., Houston, Texas.

Nuclear Magnetic Resonance (NMR) logging is creating excitement in the well logging community. Within the last year, two issues of *The Log Analyst* were devoted exclusively to NMR.[1] The *Oilfield Review* published a comprehensive article explaining borehole NMR technology less than two years ago.[2] Recently, many special workshops and conference sessions on NMR have been held by professional logging societies. Today, Internet Web sites provide current information on NMR logging advances.[3]

Why all the excitement? The reasons are clear. First, the tools used to make high-quality borehole NMR measurements have improved significantly. The quality of measurements made in the field is approaching that of laboratory instruments. Second, these measurements tell petrophysicists, reservoir engineers and geologists what they need to know—the fluid type and content in the well. The measurements also provide easy-to-use ways to identify hydrocarbons and predict their producibility. Finally, despite

the mysterious nature of the NMR technique, the measurement principles are relatively easy to understand.

Important advances have been made in applying NMR measurements to detecting and differentiating all formation fluids, such as free water and bound water, as well as differentiating gas from oil in hydrocarbon-bearing reservoirs. In this article, we review the improvements in tool technology that allow today's tools to measure different porosity components in the formation *(see "What is Sandstone Porosity, and How Is It Measured?", page 36).* Then, we evaluate the new, high-speed, cost-effective ways NMR can be used with conventional logging measurements to determine critical formation properties such as bound-water saturation and permeability for predicting production. Finally, we show how NMR measurements, in combination with other logging data, provide a more accurate, quantitative and therefore profitable understanding of formations including shaly gas sands and those containing viscous oil.

A Rapidly Developing Technology

The first NMR logging measurements were based on a concept developed by Chevron Research. Early nuclear magnetic logging tools used large coils, with strong currents, to produce a static magnetic field in the formation that polarized the hydrogen nuclei—protons—in water and hydrocarbons.[4] After quickly switching off the static magnetic field, the polarized nuclei would precess in the weak, but uniform, magnetic field of the earth. The precessing nuclei produced an exponentially decaying signal in the same coils used to produce the static magnetic field. The signal was used to compute the free-fluid index, FFI, that represents the porosity containing movable fluids.

These early tools had some technical deficiencies. First, the sensitive region for resonance signal included all of the borehole fluid. This forced the operator to use special magnetite-doped mud systems to eliminate the large borehole background signal—an expensive and time-consuming process. In addition, the strong polarizing currents would saturate the resonance receiver for long periods of time, up to 20 msec. This diminished the tool sensitivity to fast-decaying porosity components, making early tools sensitive only to the slow free-fluid parts of the relaxation decay signal. These tools also consumed huge amounts of

(continued on page 39)

1. *The Log Analyst* 37, no. 6 (November-December, 1996); and *The Log Analyst* 38, no. 2 (March-April, 1997).
2. Kenyon B, Kleinberg R, Straley C, Gubelin G and Morriss C: "Nuclear Magnetic Resonance Imaging—Technology for the 21st Century," *Oilfield Review* 7, no. 3 (Autumn 1995): 19-33.
3. The SPWLA provides an extensive bibliography of NMR publications developed by Steve Prensky, U.S. Department of Interior Minerals Management Service, located at URL: http://www.spwla.org/, and information on the Schlumberger CMR tools can be found at http://www.connect.slb.com.
The NUMAR information Web site is located at URL: http://www.numar.com.
4. Early NMR tools did not contain permanent magnets to polarize the spinning protons.

What Is Sandstone Porosity, and How Is It Measured?

Simply put, porosity is the void space in all rocks where fluids accumulate. In igneous rocks, this space is quite small because the crystallization growth process results in dominant interlocking grain contacts. Similar arguments can be made for metamorphic rocks. In contrast, sandstones are formed by the deposition of discrete particles creating abundant void space between individual particle grains.

Obviously, hydrocarbons are found only in porous formations. These rocks can be formed by the weathering and erosion of large mountains of solid rock, with the eroded pieces deposited by water and wind through various processes. As the weathered particles are carried farther from the source, a natural sorting of particle or grain size occurs *(right)*. Geology attempts to study how variations in original porosity created by different grain packing configurations are altered by post-depositional processes, whether they be purely mechanical or geochemical, or some mixture of the two.

During transportation, the smallest weathered particles of rock, such as fine-grained sands and silts, get carried the farthest. Other minerals, such as mica, which is made of sheets of aluminosilicates, break down quickly through erosion, and are also carried great distances. These sheet silicates give rise to clay minerals, which are formed by weathering, transportation and deposition. Clays can also form in fluid-filled sediments through diagenetic processes—chemical, such as precipitation induced by solution changes; or biological, such as by animal burrows; or physically through compaction, which leads to dewatering of clays. The final formation porosity is determined by the volume of space between the granular material *(next page, top)*.

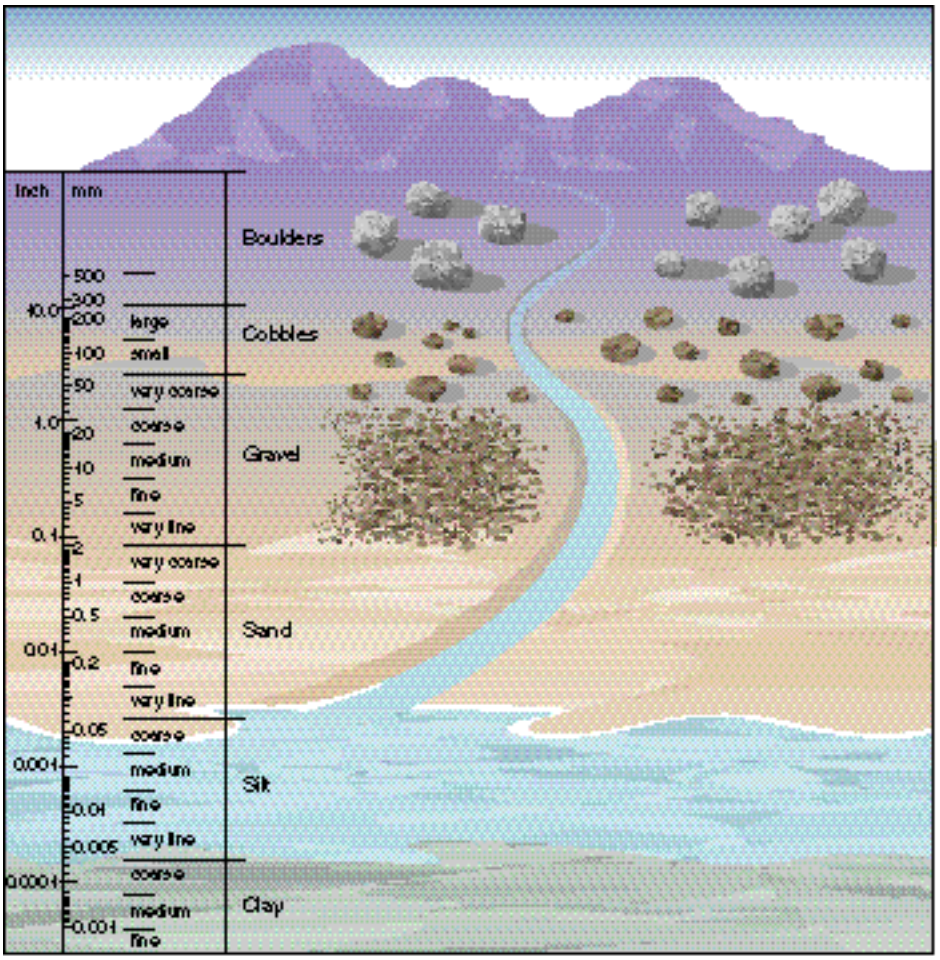

How weathering and transportation cause changes in scale of grain size. The decomposition of large rocks leads to the development of clastic sedimentary deposits. Water and wind carry the finer grained materials the farthest from their source. Many materials that are resistant to water and chemical alteration become sand and silt grains eventually deposited in sediments. Other layered-lattice minerals in the original igneous rocks, such as micas and other silicates, become transformed into fine-grained clays through degradation and hydrothermal processes.

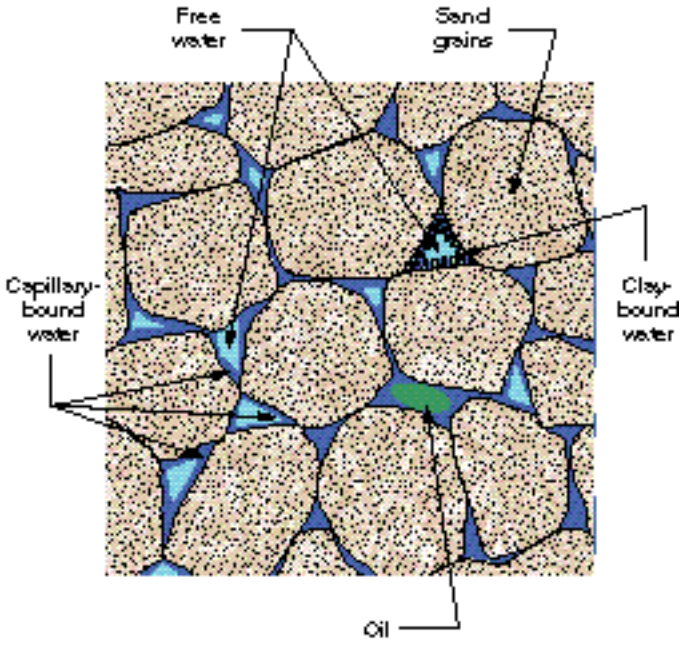

□Intergranular porosity. The pores between these water-wet sand grains are occupied by fluids and fine layers of clay. The irreducible water *(dark blue)* is held against the sand grains by surface tension and cannot be produced. Clay-bound water *(shaded dark blue)* is also unproducible. Larger pores can contain free water *(light blue)*, and in some cases there are pockets of oil *(green)* isolated from the sand grains by capillary water. The clay particles, and their associated clay-bound water layer, effectively reduce the diameter of the pore throats. This reduces the formation's ability to allow fluids to flow—permeability.

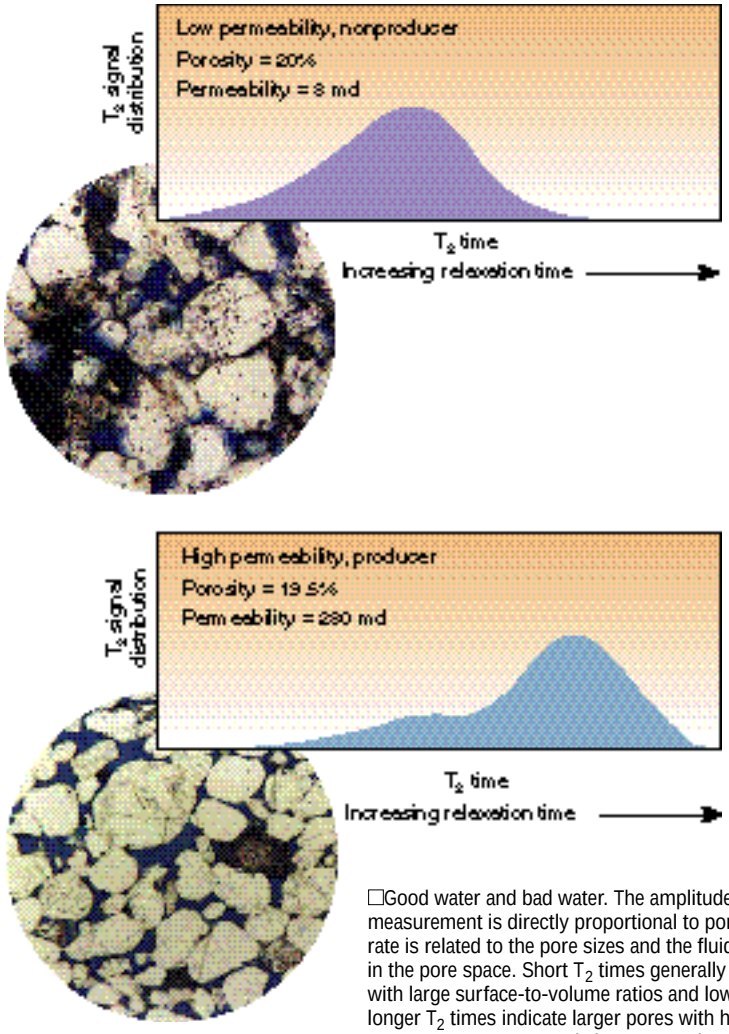

□Good water and bad water. The amplitude of the NMR T_2 measurement is directly proportional to porosity, and the decay rate is related to the pore sizes and the fluid type and viscosity in the pore space. Short T_2 times generally indicate small pores with large surface-to-volume ratios and low permeability, whereas longer T_2 times indicate larger pores with higher permeability. Measurements were made in two samples with about the same T_2 signal amplitudes, indicating similar porosity, but with considerably different relaxation times that clearly identify the sample with the higher permeability.

But, all porosity is not equivalent. Clearly, what is special about NMR is that it not only measures the volume of the void space, assuming that it is filled with a hydrogenated fluid, but also allows some inferences to be made about pore size from measurement of relaxation rates. This is the ability to apportion the porosity into different components, such as movable fluids in large pores and bound fluids in small pores.

In sandstone formations, the space surrounding pores can be occupied by a variety of different mineral grains. In the simple case of well-sorted, water-wet sandstones, water that is adhering to the surface of the sand grains is tightly bound by surface tension. Frequently, in these formations, the spaces between sand grains are filled with clay particles. Water also attaches itself to the surfaces of clay particles, and since clays have large surface-to-volume ratios, the relative volume of clay-bound water is large. This water will always remain in the formation, and is known as irreducible water. In pure sands, this is also known as capillary-bound water. All exposed mineral surfaces have adsorbed water, which link particle size with volume of irreducible water.

The NMR measurements tell us two important things. The echo signal amplitudes depend on the volume of each fluid component. The decay rate, or T_2 for each component, reflects the rate of relaxation, which is dominated by relaxation at the grain surface. T_2 is determined primarily by the pore surface-to-volume ratios. Since porosities are not equal—capillary-bound or clay-bound water are not producible, but free water is—two equal zones of porosity, but with entirely different producibility potential, can be distinguished by their T_2 time distributions *(left)*.

Hydrogen nuclei in the thin interlayers of clay water experience high NMR relaxation rates, because the water protons are close to grain surfaces and encounter the surfaces frequently. Also, if the pore volumes are small enough that the water is able to diffuse easily back and forth across the water-filled pore, then the relaxation rates will simply reflect the surface-to-volume ratio of the pores. Thus, water in small pores with larger surface-to-volume ratios has fast relaxation rates and therefore short T_2 porosity components *(next page, top left)*.

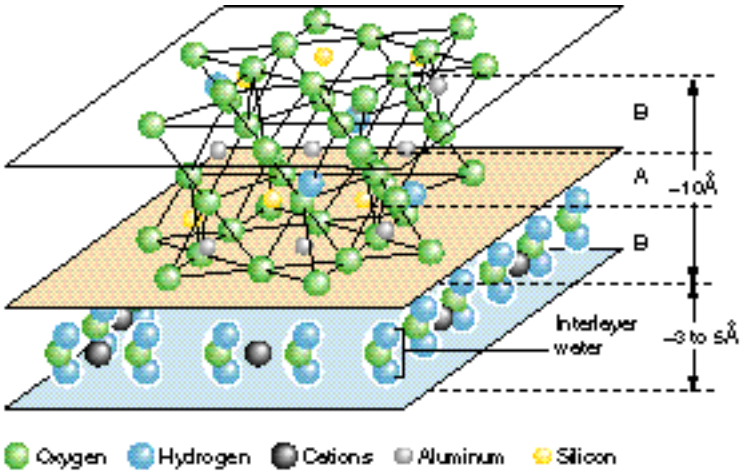

□Interlayer water and hydroxyls in clay structures. Clay minerals are hydrated silicates of aluminum which are fine grained, less than 0.002 mm. The layers are sheet structures of either aluminum atoms octahedrally coordinated with oxygen atoms and hydroxyls $[OH]^-$, or silica tetrahedral groups. These octahedral (A) and tetrahedral (B) sheets link together to form the basic lattice of clay minerals, either a two layer—one of each sheet (AB), or a three layer (BAB) structure. In smectite clay, these lattices sheets are then linked together by cations and interlayer water molecules. The hydroxyls are seen as porosity by all neutron tools, but not NMR tools. The interlayer water, trapped between sheets of the clay lattice, is not producible.

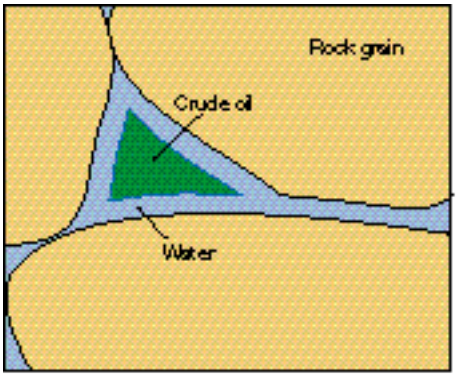

□Oil in the pore space of a water-wet rock. The lack of contact between oil and the rock grain surface allows the oil to take its bulk relaxation time, which for low-viscosity oils will generally be longer than the shortened water relaxation.

On the other hand, in large pores with smaller surface-to-volume ratios, it takes longer for the hydrogen to diffuse across the pores. This will decrease the number of encounters with the surface and lower the relaxation rate—leading to a longer T_2 component in the NMR measurement. Free water, found in large pores, is not strongly bound to the grain surfaces by surface tension. Longer T_2 time components reflect the volume of free fluid in the formation.

Another example of long T_2 time fluid components seen by NMR is the case of oil trapped inside a strongly water-wet pore *(above right)*. Here the oil molecules cannot diffuse past the oil-water interface to gain access to the grain surface. As a result, the hydrogen nuclei in the oil relax at their bulk oil rate, which is usually slow depending on the oil viscosity. This leads to a good separation of the oil and water signals in NMR T_2 distributions.[1]

Neutron tools have traditionally been used for porosity measurements. The scattering and slowing down of fast neutrons in formations lead to the detection of either thermal or epithermal neutrons, depending on the tool design. Hydrogen has an extremely large scattering cross section, and because of its mass, it is particularly effective at slowing down neutrons. Thus, the response of neutron porosity tools is sensitive to the total hydrogen concentration of the formation, which leads to their porosity response *(next page, top)*.

However, there are complications. Small differences in the other elemental neutron cross sections lead to changes in the porosity response for different minerals, called the lithology effect. There is also the effect of thermal absorbers, especially in shales, which cause large systematic increases in the porosity response of thermal neutron tools. Fortunately, epithermal neutron porosity tools, such as the APT Accelerator Porosity Tool, are immune to this effect.

Finally, because the neutrons cannot discriminate between hydrogen in the fluids or hydrogen that is an integral part of the grain structure, neutron tools respond to the total hydrogen content of the formation fluids and rocks. Even after all the clay-bound water and surface water are removed, clay minerals contain hydroxyls $[OH]^-$ in their crystal structures—kaolinite and chlorite contain $[OH]_8$ and illite and smectite contain $[OH]_4$—making them read especially high to neutron porosity tools.[2]

Density tools use gamma rays to determine porosity. Gamma ray scattering provides an accurate measurement of the average formation bulk density, and if the formation grain and fluid densities are assumed correctly, the total fluid-filled porosity can be accurately determined *(see "Gas-Corrected Porosity from Density-Porosity and CMR Measurements," page 54)*. Usually, one assumes the grain density for sandstone or limestone and water-filled pores. Errors occur if the wrong grain density is assumed—a lithology effect—or the wrong fluid density is assumed, which occurs with gas-filled pores.

Using Porosity Logs

Comparing one porosity measurement with another leads to new information about the makeup of the formation. Traditionally, neutron and density-porosity logs are combined, sometimes by simple averaging. In many cases, the lithology effects on the neutron porosity tend to cancel those on the density porosity, so that the average derived porosity is correct. If there are only two lithologies in a water or oil filled formation, then porosity and the fraction of each rock mineral can be determined using a crossplot technique. In gas zones, neutron-derived porosity reads low, if not zero, whereas density-derived porosity reads slightly high. This leads to the classic gas crossover signature—a useful feature.

NMR T_2 distributions provide for fluid discrimination. Since fluids confined to small pores near surfaces have short T_2 relaxation times and free fluids in large pores have large T_2 relaxation times, partitioning the T_2 distributions allows discrimination between the different fluid components *(next page, bottom)*. Adding the amplitudes of the observed fluid T_2 components together gives

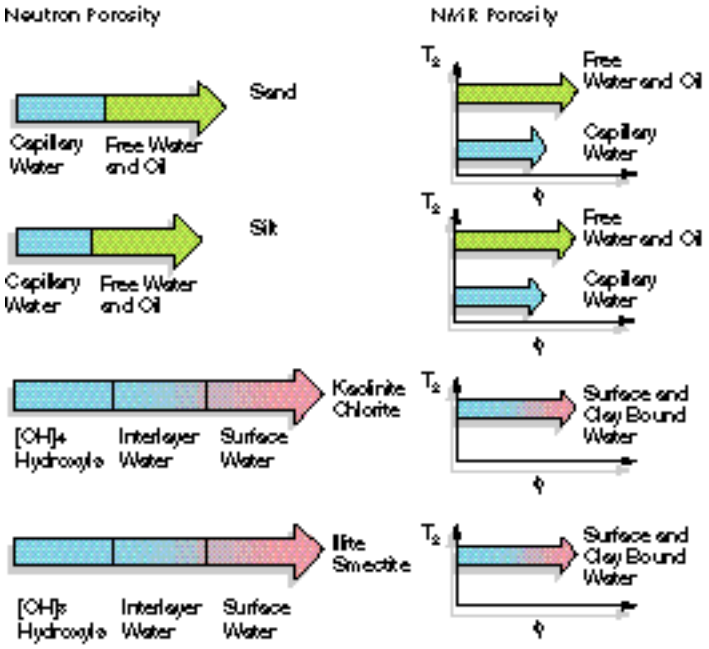

□What porosity tools measure. NMR porosity tools can discriminate between capillary-bound or clay-bound fluids by their short T_2 components and free isolated fluids with longer T_2 components *(top right)*. By contrast, neutron porosity tools are sensitive to the total hydrogen content of the formation *(left)*, and cannot distinguish between fluids of different mobility.

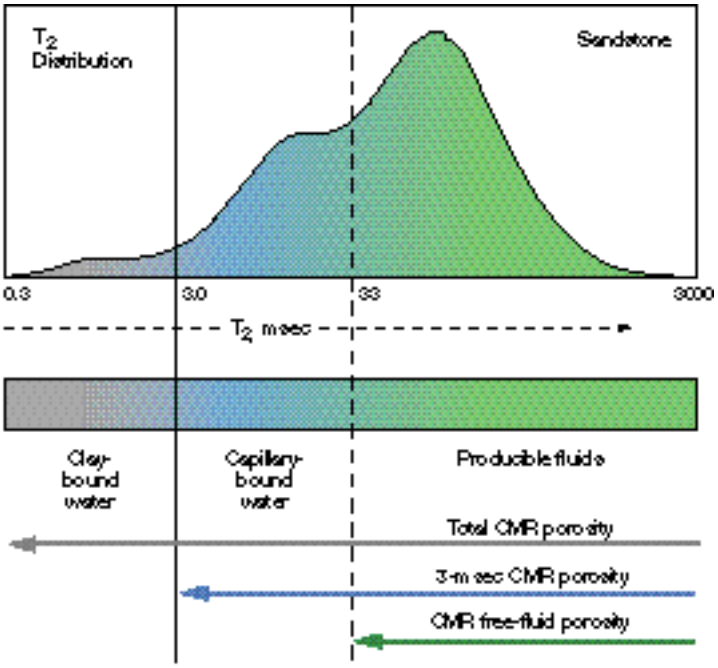

□NMR T_2 time distributions provide clear picture of the fluid components. In water-filled sandstone formations, the T_2 time distribution reflects the pore size distribution of the formation. Shorter T_2 components are from water that is close and bound to grain surfaces.

a total NMR porosity which usually agrees with the density porosity in water-filled formations. In gas zones, like the neutron porosity, NMR depends on the total hydrogen content, and therefore reads low. This leads to an NMR gas crossover signature.

1. Kleinberg and Vinegar, reference 12 main text.
2. The protons, which are part of the hydroxyls found in the clays, are so tightly bound in the crystal structure that the NMR decay is much too fast to be seen by any borehole NMR logging tool.

power to tip the polarized spinning hydrogen nuclei and were not combinable with other logging tools.

Sparked by ideas developed at Los Alamos National Laboratories in New Mexico, USA, the application of NMR technology in the oil field took a giant leap forward in the late 1980s with a new class of NMR logging tools—the pulse-echo NMR logging tools. Now, polarizing fields are produced with high-strength permanent magnets built into the tools (see *"Pulse-Echo NMR Measurements," page 44)*.[5]

Two tool styles are currently available for commercial well logging. These tools use different design strategies for their polarizing fields. To gain adequate signal strength, the NUMAR logging tool, the Magnetic Resonance Imager Log (MRIL), uses a combination of a bar magnet and longitudinal receiver coils to produce a 2-ft [60-cm] long, thin cylinder-shaped sensitive region concentric with and extending several inches away from the borehole.[6]

The Schlumberger tool, the CMR Combinable Magnetic Resonance tool, uses a directional antenna sandwiched between a pair of bar magnets to focus the CMR measurement on a 6-in. [15-cm] zone inside the formation—the same rock volume scanned by other essential logging measurements (next page).[7] Complementary logging measurements, such as density and photoelectric cross section from the Litho-Density tool, dielectric properties from EPT Electromagnetic Propagation Tool, microresistivity from the MicroSFL and epithermal neutron porosity from the APT Accelerator Porosity Tool can be used with the CMR tool to enhance the interpretation and evaluation of formation properties. Also, the vertical resolution of the CMR measurement makes it sensitive to rapid porosity variations, as seen in laminated shale and sand sequences.

5. Murphy DP: "NMR Logging and Core Analysis Simplified," *World Oil* 216, no. 4 (April 1995): 65-70.
6. Miller MN, Paltiel Z, Gillen ME, Granot J and Bouton JC: "Spin Echo Magnetic Resonance Logging: Porosity and Free Fluid Index Determination," paper SPE 20561, presented at the 65th SPE Annual Technical Conference and Exhibition, New Orleans, Louisiana, USA, September 23-26, 1990.
7. Morriss CE, Macinnis J, Freedman R, Smaardyk J, Straley C, Kenyon WE, Vinegar HJ and Tutunjian PN: "Field Test of an Experimental Pulsed Nuclear Magnetism Tool," *Transactions of the SPWLA 34th Annual Logging Symposium*, Calgary, Alberta, Canada, June 13-16, 1993, paper GGG.

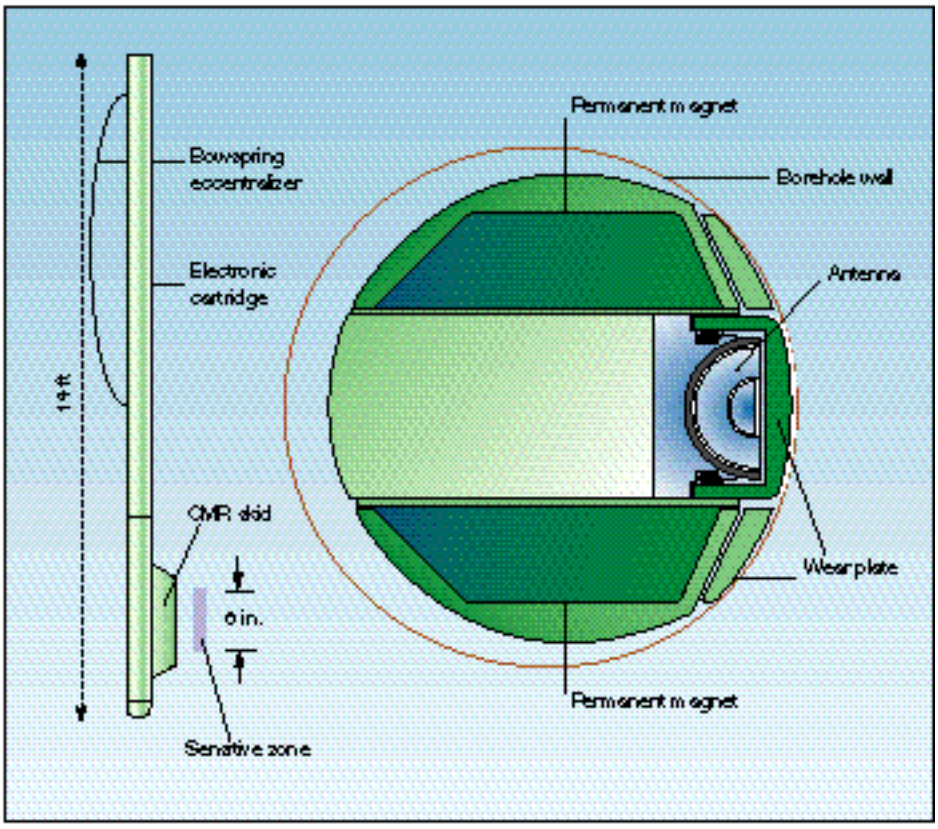

□***CMR tool. The CMR tool*** *(left)* ***is 14 ft [4.3 m] long and is combinable with many other Schlumberger logging tools. The sensor is skid-mounted to cut through mud-cake and have good contact with the formation. Contact is enhanced by an eccentralizing arm or by power calipers of other logging tools. Two strong internal permanent magnets provide a static polarizing magnetic field*** *(right)****. The tool is designed to be sensitive to a volume of about 0.5 in. to 1.25 in. [1.3 cm to 3.2 cm] into the formation and stretches the length of the antenna—about 6 in. [15 cm], providing the tool with excellent vertical resolution. The area in front of the antenna does not contribute to the signal, which allows the tool to operate in holes with a limited amount of rugosity, similar to density tools. The antenna acts as both transmitter and receiver—transmitting the CPMG magnetic pulse sequence and receiving the pulse echoes from the formation.***

NMR in the Borehole

Borehole NMR measurements can provide different types of formation porosity-related information. First, they tell how much fluid is in the formation. Second, they also supply details about formation pore size and structure that are usually not available from conventional porosity logging tools. This leads to a better description of fluid mobility—whether the fluid is bound by the formation rock or free to flow. Finally, in some cases, NMR can be used to determine the type of fluid—water, gas or oil.

The NMR measurement is a dynamic one, meaning that it depends on how it is made. Changing the wait time affects the total polarization. Changing the echo spacing affects the ability to see diffusion effects in the fluids. Transverse relaxation decay times, T_2, depend on grain surface structure, the relaxivity of the surfaces and the ability of the Brownian motion of the water to sample the surfaces. In some cases, when the pore fluids are isolated from surface contact, the observed relaxation rate approaches the bulk fluid relaxation rates.

The first pulsed-echo NMR logging tools, introduced in the early 90s, were unable to detect the fast components of the resonance decay. The shortest T_2 was limited to the 3- to 5-msec range, which allowed measurement of capillary-bound water and free fluids, together known as *effective* porosity.[8] However, clay-bound water, being more tightly bound, is believed to decay at a much faster rate than was measurable with these tools. Within the last year, improvements in these tools enable a factor-of-ten faster decay rate measurement. Now measuring T_2 decay components in the 0.1 to 0.5 msec range is possible. These improvements include electronic upgrades, more efficient data acquisition and new signal-processing techniques that take advantage of the early-time information.

For example, NUMAR added a multiplexed timing scheme to their standard tools to boost the signal-to-noise ratio for fast-decay modes. This was achieved by combining a standard pulse-echo train—consisting of 400 echoes with an echo spacing of 1.2 msec—and a rapid burst of short echo trainlets of 8 to 16 echoes with half the standard echo spacing.[9] This pulse sequence is repeated 50 times to reduce the noise by a factor of seven. Now, this tool is sensitive to transverse decay components with T_2 as short as 0.5 msec.

The Schlumberger CMR tool has also had hardware improvements and signal-processing upgrades.[10] The signal-to-noise per echo has been improved by 50% in the new resonance receiver. Also, the echo acquisition rate has been increased 40%, from 0.32-msec spacing to 0.2 msec, increasing the CMR ability to see fast decay times *(next page)*. In addition, the signal-processing software has been optimized for maximum sensitivity to the short T_2 decays. As a result, a new pulsed-echo tool, called the CMR-200 tool, can measure formation T_2 components as short as 0.3 msec in continuous logging modes and as short as 0.1 msec in stationary logging modes.

Total Porosity

NMR measurements now have the ability to see more of the fluids in the formation, including the sub-3-msec microporosity associated with silts and clays, and intraparticle porosity found in some carbonates. Therefore, the measurement provided by NMR tools is approaching the goal of a lithology-independent *total porosity* measurement for evaluating complex reservoirs.

Total porosity using NMR T_2 decay amplitudes depends on the hydrogen content of the formation, so in gas zones, NMR poros-

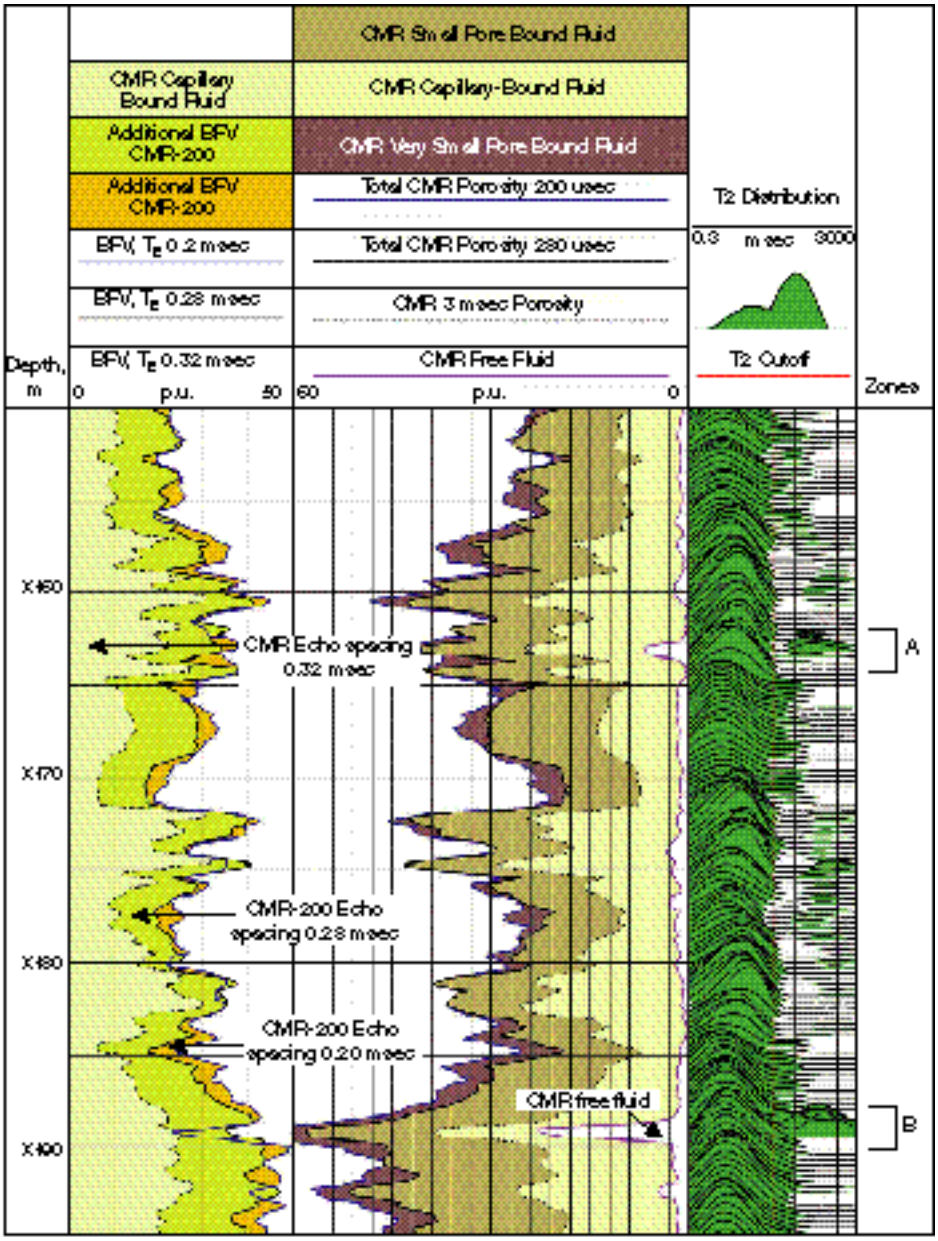

☐How increased echo rate improves CMR ability to see early-time decay from small pores. CMR tool was run in a shallow Cretaceous Canadian test well at three different echo spacings—0.32 msec, 0.28 msec and 0.20 msec. As echo spacings decrease, the total observed porosity (middle track) read by the tool increases in the shaly intervals, containing small pores, because the ability to see the sub-3 msec T_2 components (right track) increases with echo rate. This is verified by the increased CMR-200 bound fluid volume (BFV) curves (left track). In the two sand zones A and B, the long T_2 components seen in the time distributions correspond to increases in observed CMR free fluid (middle track).

ity reads low because the hydrogen density in gas is less than in water or oil and there is incomplete gas polarization. The difference between total NMR porosity and density porosity logs provides an indicator of gas.

Other applications based on NMR porosity discrimination are permeability logs and irreducible water saturation. In the future, the improved T_2 sensitivity of NMR porosity logs may permit accurate estimates of clay-bound-water volumes for petrophysical interpretation, such as the calculation of hydrocarbon saturation through Dual-Water or Waxman-Smits models.

A simple example from South America illustrates the improved sensitivity to shale resulting from the increased ability to measure fast-decay components *(next page, top left)*. Density-derived porosity was calculated assuming a sandstone matrix density of 2.65 g/cm^3, and thermal neutron porosity was computed also assuming a sandstone matrix.

The CMR-200 T_2 distributions shown in track 3 were used to compute total porosity, TCMR; a traditional CMR 3-msec effective porosity curve, CMRP, shown in track 2; and a 12-msec bound-fluid porosity BFV curve, based on the fast-decaying portion of the T_2 distribution, shown in track 1.

All the porosity logs in track 2 agree in Zone B, indicating a moderately clean water-filled sandstone reservoir. This shale-free zone makes relatively little contribution to the relaxation time distribution below the 3-msec detection limit of the early pulse-echo CMR tools. However, in the shale, Zone A, the picture changes. Here, the bulk of the porosity T_2 response shifts to a much shorter part of the T_2 distribution that is easily seen in track 3. In the shale zone, the new CMR-200 total porosity curve in track 2 is sensitive to the fast-decaying components and agrees well with the density porosity. The older CMR 3-msec porosity in track 2 misses the fast-decaying components of the T_2 distribution between 0.3 and 3 msec, and therefore reads 10 p.u. lower in the shale zone.

The large sub-3-msec porosity contribution suggests that the shales contain clay minerals with a high bound-water content.

8. Miller et al, reference 6.
9. Prammer MG, Drack ED, Bouton JC, Gardner JS, Coates GR, Chandler RN and Miller MN: "Measurements of Clay-Bound-Water and Total Porosity by Magnetic Resonance Logging," paper SPE 36522, presented at the 1996 SPE Annual Technical Conference and Exhibition, Denver, Colorado, USA, October 6-9, 1996.

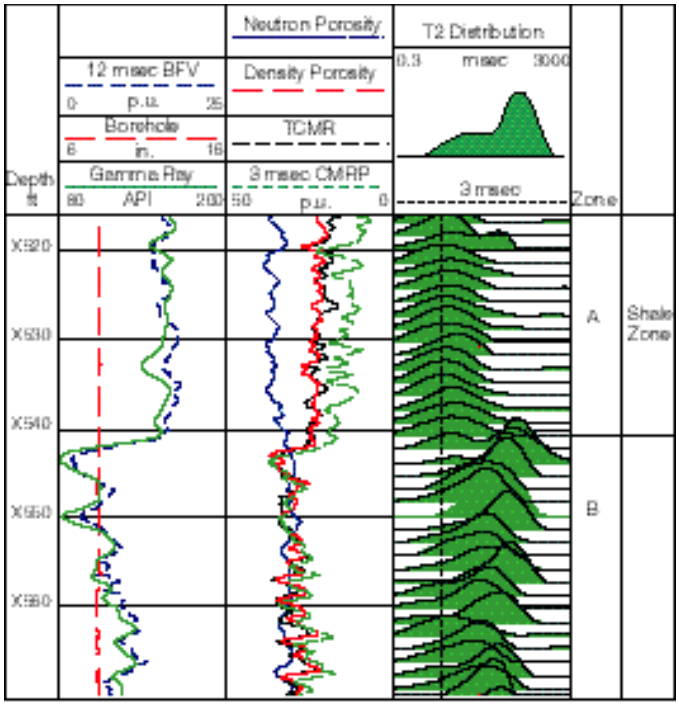

□*Total porosity logging with the PLATFORM EXPRESS tool differentiates sands and shales. The porosity logs are shown in track 2 of the wellsite display. Both neutron and density porosity were derived assuming a sandstone matrix. Total CMR porosity (TCMR) correctly finds the tightly bound shale porosity seen in the short T_2 distributions shown in track 3. The neutron porosity log reads too high in the shale interval, Zone A, due to neutron absorbers in the shale. The gamma ray and bound-fluid porosity, BFV (all porosity with T_2 below 12 msec) in track 1 show that the CMR measurement provides an alternative method for identifying shale zones.*

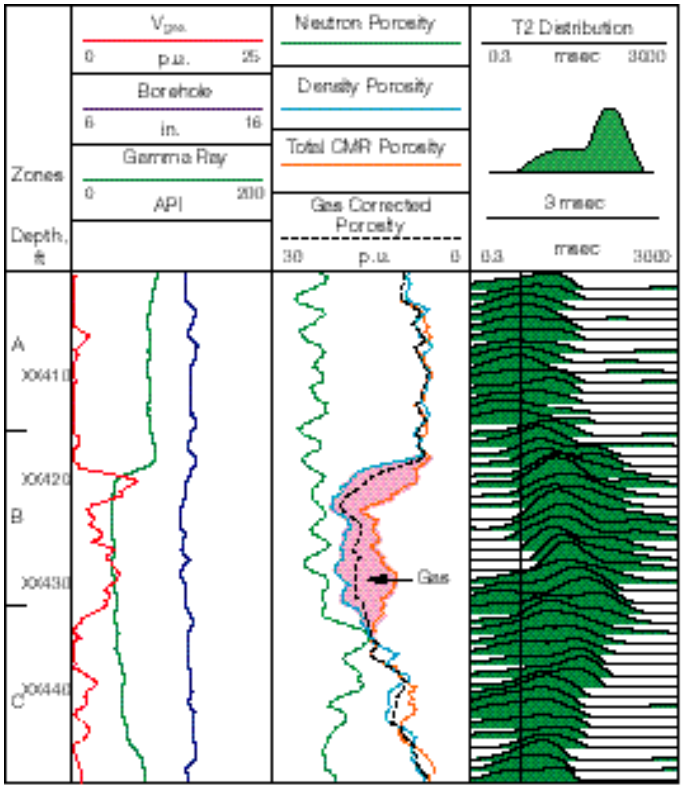

□*Using total CMR porosity and density to find gas. In track 2 the deficit between total porosity (red curve) and density porosity (blue curve) in a shaly sand can be used to identify a gas zone. The traditional neutron-density crossover is suppressed by the shaliness, which opposes the gas effect in the thermal-neutron log (green curve). The T_2 time distributions show large contributions from short relaxation times below 3-msec coming from the clay-bound water in the shales. The gas corrected porosity, (dashed black curve) is always less than the density porosity and greater than the total CMR porosity.*

The thermal neutron log is reading too high in the shale zone because of the large thermal absorption cross section of the shale, probably caused by some trace absorption elements such as boron or gadolinium associated with the clays.

In track 1, there is a strong correlation between the gamma ray log and the bound-fluid porosity curve, BFV, obtained using everything below a 12-msec T_2 cutoff. This suggests another interesting application for total porosity measurements—the porosity associated with short T_2 components can provide a good shale indicator that is independent of natural radioactivity in the formation. This is significant because there are many important logging environments with clean sands that contain radioactive minerals. In these environments, gamma ray logs are not useful for differentiating sands and shales. At best, gamma ray logs are only qualitative shale indicators, and are usually used to estimate clay corrections used for computing effective porosity.

Finding Gas in Shaly Sands—A south Texas well illustrates the value of total CMR porosity logging in detecting gas in shaly sand formations. The interval consists of a shale overlying a shaly gas sand *(above right)*. Looking for gas with the traditional thermal neutron-density crossover is unreliable or impossible in shaly formations, because thermal neutron absorbers in shales force the thermal neutron porosity tools to read too high—as can be seen in this example. This effect on the neutron log suppresses the gas signature, which means the neutron-porosity curve never consistently drops below the density-porosity curve when the logging tools pass a gas zone.

Fortunately, total porosity NMR logging works well in these environments, simplifying the interpretation. Starting from the bottom of the interval, in the lower sand, Zone C, the total CMR porosity TCMR agrees with the density porosity. However, in Zone B at the top of this shaly sand, the CMR-derived porosity drops, crossing below the density-derived porosity. This is the NMR-density logging crossover—a gas signature. The NMR porosity signal drops in the gas zone due to the reduced concentration of hydrogen in the gas and long gas polarization time—leading to incomplete polarization of the gas. The logged density-derived porosity, which assumed water-filled pores, reads slightly high in the gas zone—accentuating the crossover effect. Since gas affects both CMR porosity and density porosity, the CMR-based gas signature works effectively in shaly sands.

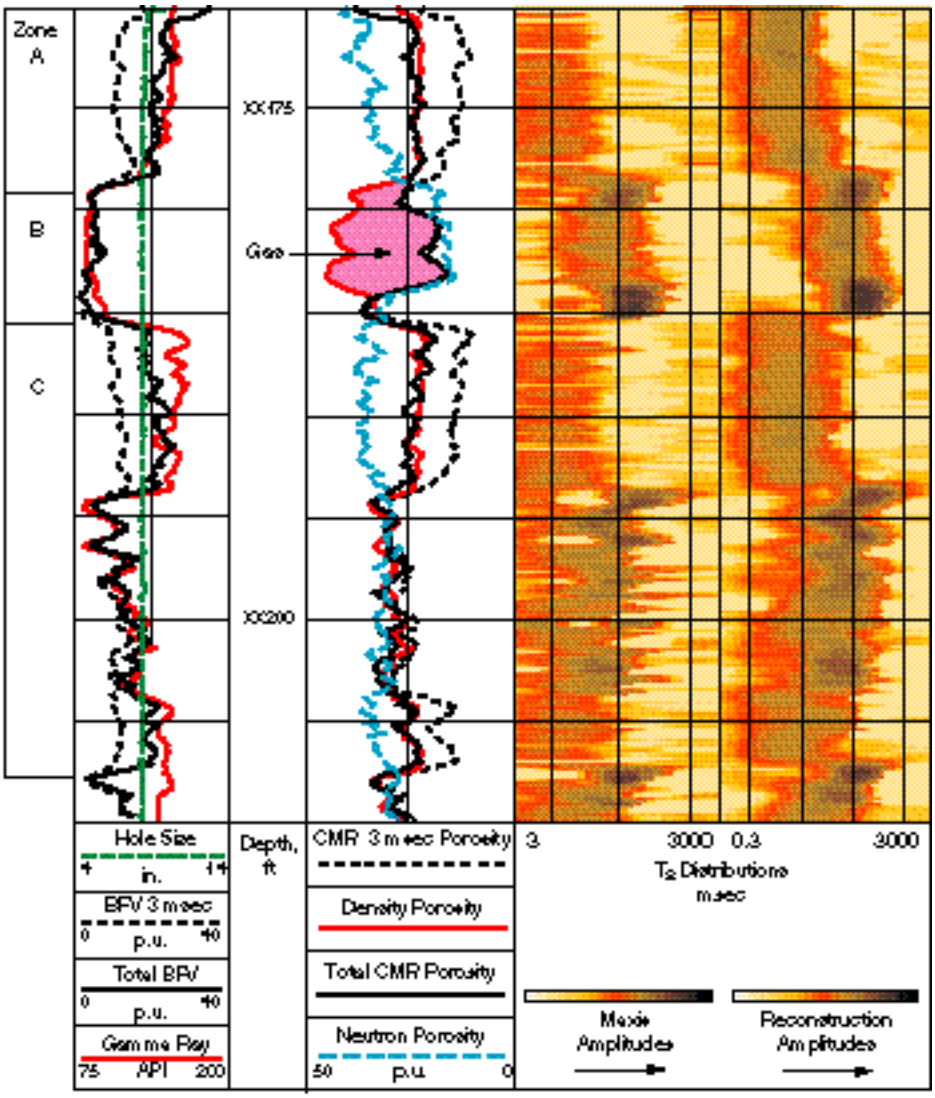

□*Detecting gas using total porosity logging with the PLATFORM EXPRESS tool. A dramatic improvement in agreement between the CMR-200 total porosity (solid black), compared to the 3-msec CMR porosity (dotted black), and density porosity (red), shown in track 2, is obtained by including the fast-decaying shale-bound porosity components from the new CMR-200 T_2 distribution shown in track 4. This enhances the ability to use the CMR total porosity and density-porosity crossover as a flag to detect gas—pink-shaded area in track 2. Improvements in the signal processing are obvious when the CMR-200 total bound-fluid log (solid black) is compared to the old 3 msec CMR bound-fluid log (dotted black) shown in track 1.*

Based on the petrophysical responses for CMR total porosity and density porosity, a new gas-corrected porosity $\varphi_{gas\text{-}corr}$, shown in track 2, and the volume of gas V_{gas}, shown in track 1, are derived *(see "Gas-Corrected Porosity from Density-Porosity and CMR Measurements," page 54)*.[11] The new gas-corrected porosity, computed from the TCMR and density-porosity shown in track 2, gives a more accurate estimate of true porosities in the gas zones. NMR works here, where the traditional neutron tool doesn't, because NMR porosity responds only to changes in hydrogen concentration, and not to neutron absorption in the shales. In the shale, Zone A, the total CMR and gas-corrected porosities again agree with the density-porosity curve, as expected.

Finally, in the lowest interval, Zone C, below the gas sand, there is a transition into poorer-quality sand with lower permeability as evidenced by the short relaxation times seen in the T_2 distributions. This zone shows little indication of gas because the total CMR porosity, gas-corrected porosity and density-porosity logs are in agreement.

Another striking example, from a British Gas well in Trinidad, shows how the CMR-derived total porosity was used with density-derived porosity to detect gas in shaly sands *(left)*. The interval contains shaly water zones at the bottom, Zone C, followed by a thin, 6-ft [2-m] clean sand, Zone B, topped by a section of shale, Zone A. There is a gas-water contact at XX184 ft in the lower part of the clean sand in Zone B. The CMR total porosity curve, shown in track 2, overlies the density-porosity curve throughout the water-filled shaly sand intervals. In the clean sand, which contains gas, there is a large separation between the CMR total porosity and the density-porosity curves. Again, the reduction in the CMR porosity response is due to the reduced concentration of hydrogen in the gas. The large crossover of these two logs provides a clear flag for finding gas in the reservoir.

The NMR logs shown in this example were obtained with the early pulse-echo CMR tool. Comparing the early tool's 3-msec effective porosity log with the new total porosity log demonstrates the improvement provided by the new CMR total porosity algorithms. The total porosity and effective porosity curves, shown in track 2, are similar in the clean sand, but the 3-msec porosity log misses the fast-decaying porosity in the shale zones. Similarly, the bound-fluid porosity log based on the early tool's 3-msec limited T_2 distributions, shown in track 3, is much noisier and misses most of the bound-fluid porosity in the shale zones. The new CMR T_2 distributions in track 4 show large contributions from the fast-decaying shale with bound-fluid components between 0.3 and 3 msec. Like the previous example, the new total porosity-derived bound-fluid log now correlates well with the gamma ray, and can be used as a improved shale indicator. As commercial CMR tools are upgraded to CMR-200 hardware, logging data and interpretation results, like those in this example, will improve.

(continued on page 46)

10. Freedman R, Boyd A, Gubelin G, Morriss CE and Flaum C: "Measurement of Total NMR Porosity Adds New Value to NMR Logging," *Transactions of the SPWLA 38th Annual Logging Symposium*, Houston, Texas, USA, June 15-18, 1997, paper 00.
11. Bob Freedman, personal communication, 1997.

A feature common to second-generation NMR logging tools is the use of an advanced pulse-echo spin flipping scheme designed to enhance the measurement. This scheme, first developed nearly fifty years ago for laboratory NMR measurements, works in the following way.[1]

The Source —All hydrogen nuclei in water [H_2O]; gas such as methane [CH_4]; and oil [C_nH_m] are single, spinning, electrically charged hydrogen nuclei—protons. These spinning protons create magnetic fields, much like currents in tiny electromagnets.

Proton Alignment—When a strong external magnetic field—from the large permanent magnet in a logging tool—passes through the formation with fluids containing these protons, the protons align along the polarizing field, much like tiny bar magnets or magnetic compass needles. This process, called polarization, increases exponentially in time with a time constant, T_1.[2]

Spin Tipping—A magnetic pulse from a radio frequency antenna rotates, or tips, the aligned protons into a plane perpendicular to the polarization field. The protons, now aligned with their spin axis lying in a plane transverse to the polarization field, are similar to a spinning top tipped in a gravitational field, and will start to precess around the direction of the field. The now-tipped spinning protons in the fluid will precess around the direction of the polarization field produced by the permanent magnet in the logging tool *(above)*.

The Effects of Precession—The precession frequency, or the resonance frequency, is called the Larmor frequency and is proportional to the strength of the polarization field. The precessing protons, still acting like small magnets, sweep out oscillating magnetic fields just as many radio antennas transmit electromagnetic fields. The logging tools have receivers connected to the same antennas used to induce the spin-flipping pulses. The antennas and receivers are tuned to the Larmor frequency—about 2 MHz for the CMR tool—and receive the tiny radio frequency signal—a few microvolts—from the precessing protons in the formation.

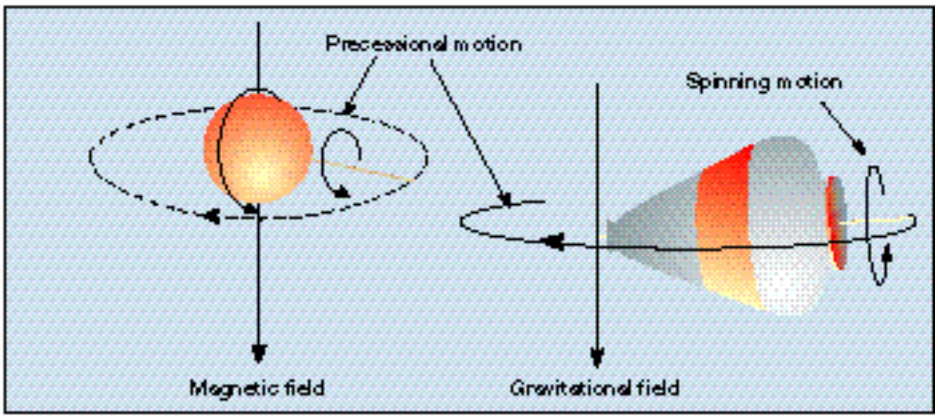

□Precessing protons. Hydrogen nuclei—protons—behave like spinning bar magnets. Once disturbed from equilibrium, they precess about the static magnetic field *(left)* in the same way that a child's spinning top precesses in the Earth's gravitational field *(right)*.

A Faint Signal from the Formation—In a perfect world, the spinning protons would continue to precess around the direction of the external magnetic field, until they encountered an interaction that would change their spin orientation out of phase with others in the transverse plane—a transverse relaxation process. The time constant for the transverse relaxation process is called T_2, the transverse decay time. Measuring the decay of the precessing transverse signal is the heart of the NMR pulse-echo measurement.

Unfortunately, it is not a perfect world. The polarization field is not exactly uniform, and small variations in this polarization field will cause corresponding variations in the Larmor precession frequency. This means that some protons will precess at different rates than others. In terms of their precessional motion, they become phase incoherent and will get out of step and point in different directions as they precess in the transverse plane *(next page)*. As the protons collectively get out of step, their precessing fields add together incoherently, and the resonance signal decays at an apparent rate much faster than the actual transverse relaxation rate due to the dephasing process described above.[3]

Spin-Flipping Produces Pulse Echoes—A clever scheme is used to enhance the signal and to measure the true transverse relaxation rate by *reversing* the dephasing of the precessing protons to pro-

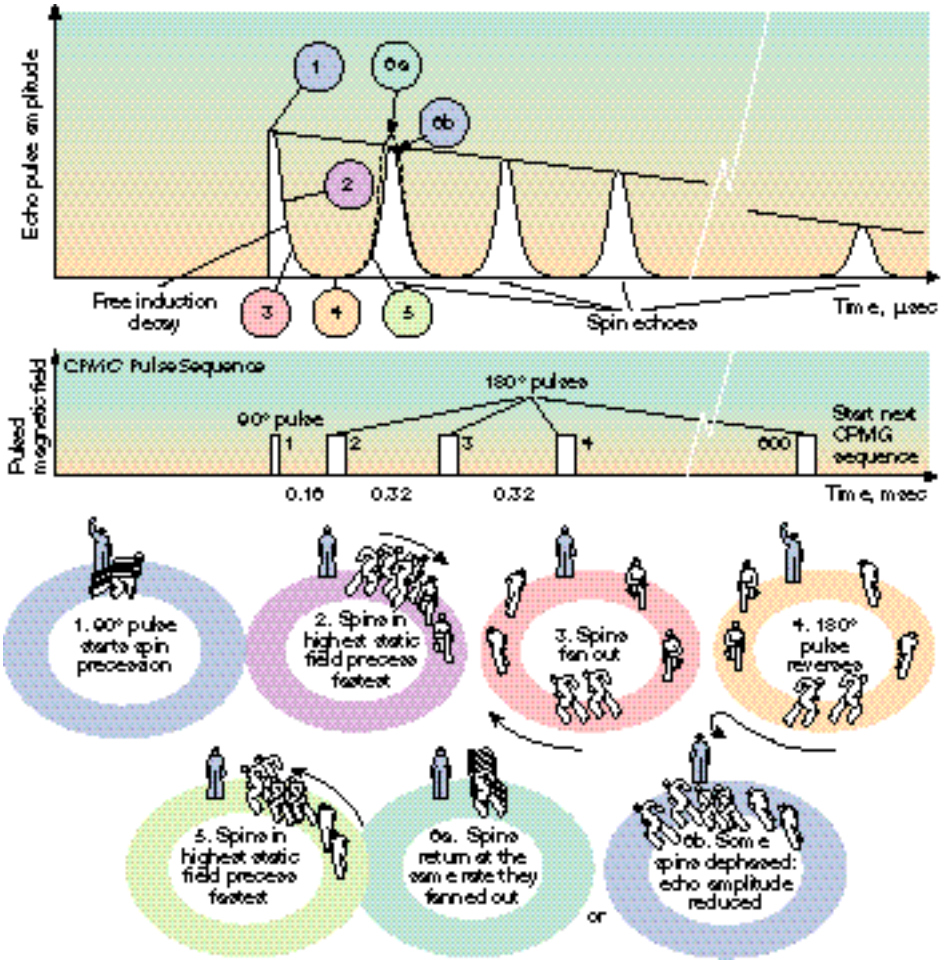

□Pulse-echo sequence and refocusing. Each NMR measurement comprises a sequence of transverse magnetic pulses transmitted by an antenna—called a CPMG pulse-echo sequence *(middle)*. Each CPMG sequence starts with a pulse that tips the protons 90° and is followed by several hundred pulses that refocus the protons by flipping them 180°. This creates a refocusing of the dephased spins into an echo. The reversible fast decay of each echo—the free induction decay—is caused by variations in the static magnetic field *(top)*. The irreversible decay of the echoes—as each echo peak decays relative to the previous one—is caused by molecular interactions and has a characteristic time constant of T_2—transverse relaxation time. The circled numbers correspond to steps numbered in the race analogy.

Imagine runners lined up at the start of a race *(bottom)*. They are started by the 90° pulse (1). After several laps, the runners are spread around the track (2, 3). Then the starter fires a second pulse of 180° (4, 5) and the runners turn around and head in the other direction. The fastest runners have the farthest distance to travel and all of them will arrive at the same time if they return at the same rate (6a). With any variation in speed, the runners arrive back at slightly different times (6b). Like the example of runners, the process of spin reversals is repeated hundreds of times during an NMR measurement. Each time the echo amplitude is less and the decay rate gives T_2 relaxation time.

duce what is called a spin echo. This is done applying a 180° *spin flipping* magnetic pulse a short time—at half the echo spacing—after the spins have been tipped into the transverse plane and have started to dephase. By flipping the spins 180°, the protons continue to precess, in the same transverse plane as before, but now the slowest one is in first and the fastest one last. Soon the slowest ones catch up with the fastest, resulting in all spins precessing in phase again and producing a strong coherent magnetization signal (called an echo) in the receiver antenna. This process, known as the pulse-echo technique, is repeated many times; typically 600 to 3000 echoes are received in the CMR tool.

***The T_2 Resonance Decay*—The pulse-echo technique used in today's logging tools is called the CPMG sequence, named after Carr, Purcell, Meiboom and Gill who refined the pulse-echo scheme.[4] It compensates for the fast decay caused by reversible dephasing effects. However, each subsequent echo will have an amplitude that is slightly smaller than the previous one because of remaining *irreversible* transverse relaxation processes.**

***Irreversible Relaxation Decay Rates*—Measuring echo amplitudes determines their transverse magnetization decay rate. The time constant T_2 characterizes the transverse magnetization signal decay. The decay comes from three sources;**

- **intrinsic – the intrinsic bulk relaxation rate in the fluids,**
- **surface – the surface relaxation rate, a formation environmental effect**
- **diffusion – the diffusion-in-gradient effect, which is a mix of environmental and tool effects.**

Bulk-fluid relaxation is caused primarily by the natural spin-spin magnetic interactions between neighboring protons. The relative motions of two spins create a fluctuating magnetic field at one spin due to the motion of the other. These fluctuating magnetic fields cause relaxation. The interaction is most effective when the fluctuation occurs at the Larmor frequency, 2 MHz for the CMR tool—a very slow motion on the molecular time scale.

Molecular motions in water and light oils are much more rapid, so the relaxation is very inefficient with long decay times. As the liquids become more viscous, the molecular motions are slower, and therefore are closer to the Larmor frequency. Thus viscous oils relax relatively effi-

1. Hahn EL: "Spin Echoes," *Physical Review* 80, no. 4 (1950): 580-594.
2. The time constant for this process, T_1, is frequently known as the spin-lattice decay time. The name comes from solid-state NMR, where the crystal lattice gives up energy to the spin-aligned system.
3. The observed fast decay due to the combined components of irreversable transverse relaxation decay interactions and the reversable dephasing effect is frequently called the *free induction decay*.
4. Carr HY and Purcell EM: "Effects of Diffusion on Free Precession in Nuclear Magnetic Resonance Experiments," *Physical Review* 94, no. 3 (1954): 630-638.
   Meiboom S and Gill D: "Modified Spin-Echo Method for Measuring Nuclear Relaxation Times," *The Review of Scientific Instruments* 29, no. 8 (1958): 688-691.

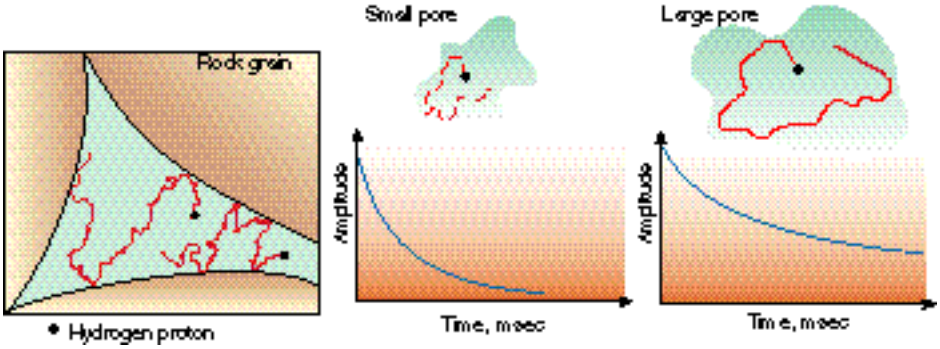

□Grain surface relaxation. Precessing protons diffuse about the pore space colliding with other protons and with grain surfaces *(left)*. Every time a proton collides with a grain surface there is a possibility of a relaxation interaction occurring. Grain surface relaxation is the most important process affecting relaxation times. Experiments show that when the probability of colliding with a grain surface is high—in small pores *(center)*—relaxation is rapid and when the probability of colliding with a grain surface is low—in large pores *(right)*—relaxation is slower.

ciently with short T_1 and T_2 decay times *(right)*. It should be noted that for liquids with viscosity less than 1 cp, T_2 does not change much—and even decreases for low viscosity. This is due to the diffusion-in-gradient mechanism, which is strongest for liquids with the largest diffusion coefficient—lowest viscosity. This effect is also enhanced by long echo spacing. The diffusion-in-gradient mechanism does not affect T_1.[5]

Fluids in contact with grain surfaces relax at a much higher rate than their bulk rate. The surface relaxation rate depends on the ability of the protons in the fluids to make multiple interactions with the surface. For each encounter with the grain surface, there is a high probability that the spinning proton in the fluid will be relaxed through atomic-level electromagnetic field interactions. For the surface process to dominate the overall relaxation decay, the protons in the fluid must make many random diffusion (Brownian motion) trips across the pores in the formation *(above)*. They collide with the grain surface many times until a relaxation event occurs.

Finally, there is relaxation from diffusion in the polarization magnetic field gradient. Because protons move around in the fluid, the compensation by the CPMG pulse-echo sequence is never complete. Some protons will drift into a different field strength during their motion between *spin flipping* pulses, and as a result they will not receive correct phase adjustment for their previous polarization field environment. This leads to a further, though not significantly large, increase in the T_2 relaxation

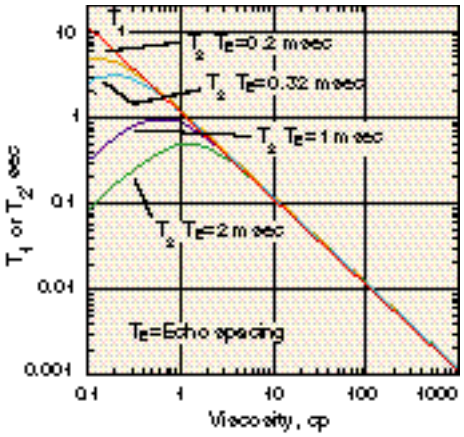

□Relaxation time versus viscosity. The bulk relaxation of crude oil can be estimated from its viscosity at reservoir conditions. T_2 values are shown for various echo spacings and have been computed for the CMR tool with a 20 gauss/cm magnetic field gradient. Diffusion-in-gradient effects, which depend on echo spacing, T_E, dominate T_2 rates for low viscosity liquids.

rates for water and oil. Gas, because of its high diffusion mobility, has a large diffusion-in-gradient effect. This is used to differentiate gas from oil.[6]

The pulse-echo measurements are analyzed in terms of multiple exponentially decaying porosity components. The amplitude of each component is a measure of its volumetric contribution to porosity.

5. Kleinberg RL and Vinegar HJ: "NMR Properties of Reservoir Fluids," *The Log Analyst* 37, no. 6 (November-December, 1996): 20-32.

6. Akkurt R, Vinegar HJ, Tutunjian PN and Guillory AJ: "NMR Logging of Natural Gas Reservoirs," *The Log Analyst* 37, no. 6 (November-December, 1996): 33-42.

Total Porosity for Better Permeability Answers—In the North Sea, micaceous sandstones challenge density-derived porosity interpretation and permeability analysis, because grain densities are not well-known. Here, CMR-derived total porosity provides a much better match to core porosity than conventional porosity logging tools *(next page, top)*. In addition, permeability data derived from CMR measurements are of considerable value. Other sources of measuring this critically important reservoir parameter, such as coring and testing, invoke high cost or high uncertainty.

Experience in these environments shows that wellsite computations of CMR porosity and permeability using the default parameters agree well with core data in at least 75% of wells. Typically, default parameters assume a fluid-hydrogen index of unity (for water) and the Timur-Coates equation with a 33-msec T_2 cutoff is used for computing the bound-fluid log.[12] In most of these wells, the CMR tool is now being used to replace some of the coring, especially in frontier offshore drilling operations where coring can cost up to $6000 per meter.

An offshore Gulf of Mexico gas well, drilled with oil-base mud on the flank of a large salt dome, provided an opportunity to evaluate fluid contacts in an established oil and gas field and determine hydrocarbon productivity in low-resistivity zones. Previous deep wells on this flank encountered drilling difficulties leading to poor-to-fair boreholes and degraded openhole log quality. This resulted in ambiguous petrophysical analysis and reservoir characterization.

The combination of CMR measurements and other logs provides a straightforward description of the petrophysics in this well *(next page, bottom)*. These logs show many high-resistivity zones in track 2 and density-neutron crossovers in track 3, which signal these intervals as potentially gas-producing. Total CMR porosity is low in the gas intervals. There are some low-resistivity intervals that could produce free water. Of special interest are the low-resistivity zones at the base of the gas sand in Zone C, which may indicate a water leg, and the low-resistivity sand in Zone D. The CMR bound-fluid porosity increases in these zones.

An ELAN Elemental Log Analysis interpretation, which combines resistivity and CMR

12. The hydrogen index is the volume fraction of fresh water that would contain the same amount of hydrogen. The Timur-Coates equation is a popular formula for computing permeability from NMR measurements. Its implementation uses ratio of the free-fluid to bound-fluid volumes. It was first introduced in Coates G and Denoo S: "The Producibility Answer Product," *The Technical Review*, 29, no. 2 (1981): 54-63.

Permeability logging using CMR total porosity in North Sea micaceous sandstones. A good match (track 2), between core- and CMR-derived permeability using the default Timur-Coates equation, is common in many North Sea reservoirs. This example is from an oil zone drilled with oil base mud.

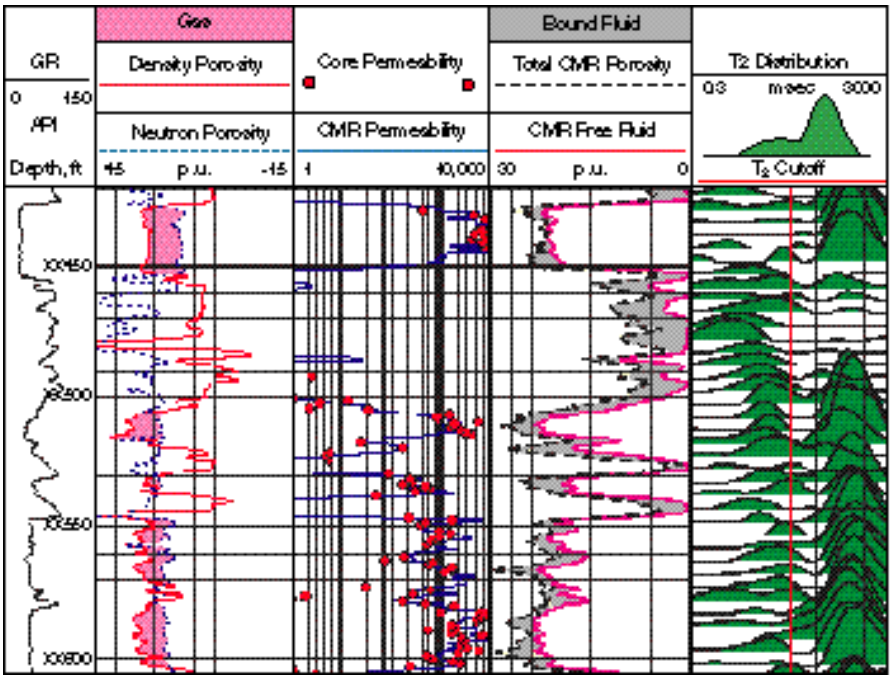

Gas production in the Gulf of Mexico. Bimodal CMR T_2 distributions in track 4 show effects of oil-base mud invasion with long T_2 and large bound-fluid components below the 33-msec T_2 cutoff. Neutron-density crossover clearly shows gas zones. The low CMR signal is due to the low hydrogen content and long polarization time of the gas. The bound-fluid measurement was used with the resistivity data to determine movable water in the lower resistivity zones.

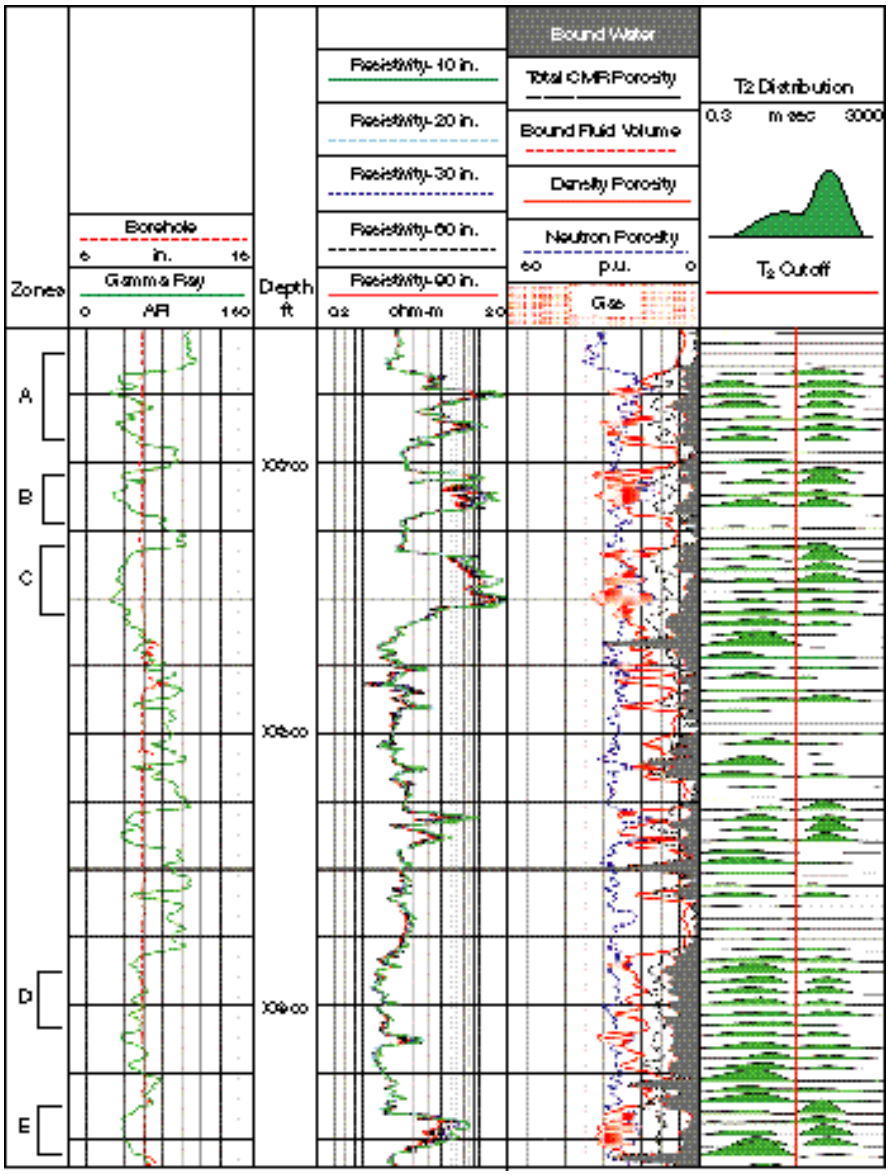

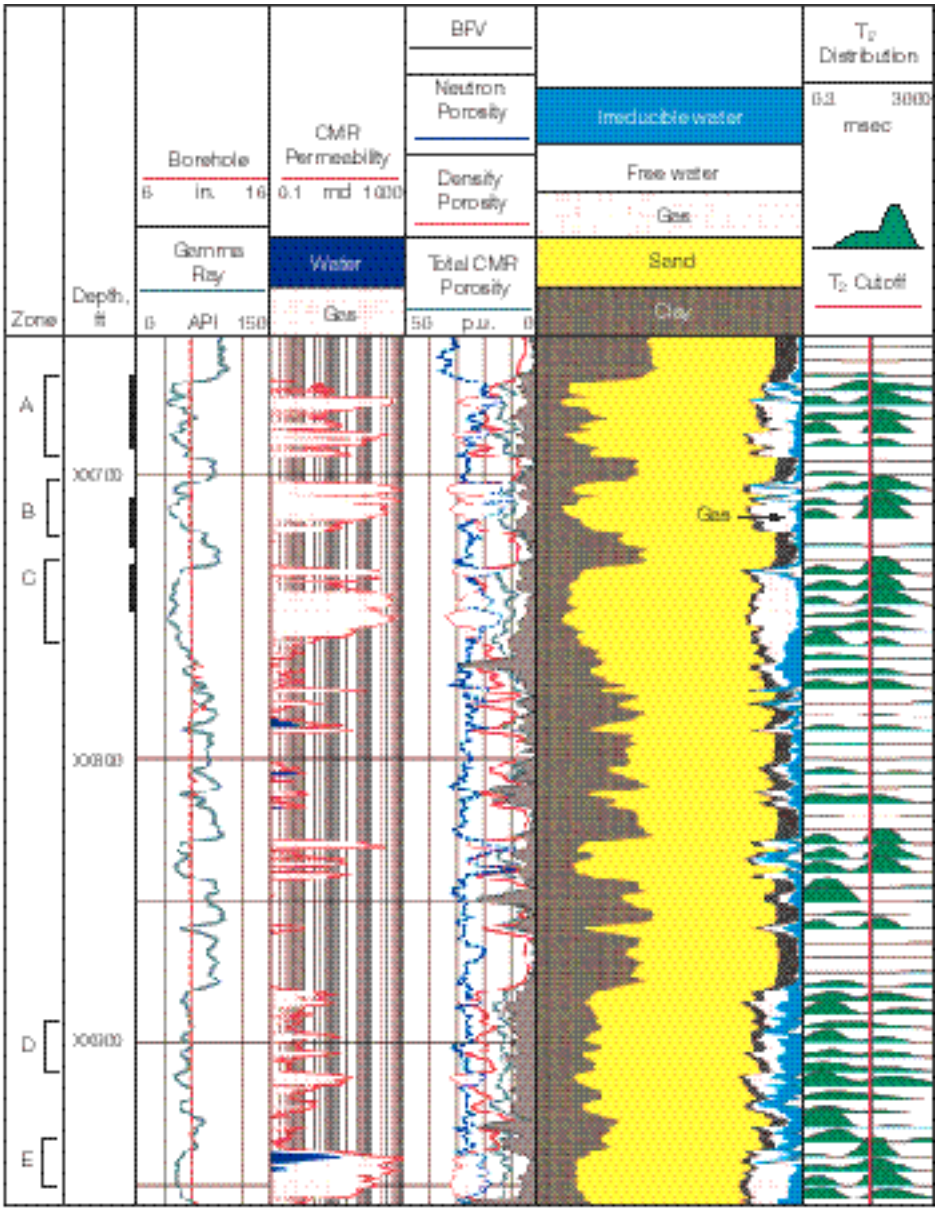

□ELAN interpretation analysis. The CMR-resistivity interpretation suggests that there is no movable water in the entire logged interval. The top three sand zones A, B and C, all with high permeability determined by the CMR tool, track 2, produced 20 MMcf/D of gas with 780 B/D condensate and no water. The reserves indicated in the lower sand Zone E will be completed at a later time.

data, shows that there is little free water in this entire interval *(left)*. Most of the water contained in these zones appears irreducible because the CMR bound-fluid volume matches the total water volume derived from the resistivity logs. The upper three sands were completed and the CMR total porosity, bound-fluid and permeability logs allowed the operator to confidently perforate Zones A, B and C.[13] The initial production from the upper three sand zones was 20 MMcf/D, 780 B/D [124 m^3/d] of condensate with less than 1% water, confirming the CMR interpretation. The lower sands, Zones D and E, have not been completed because of downdip oil production. However, the interpretation results from these zones have been included in the overall well reserves analysis.

Another Gulf of Mexico example from an infill development well in a faulted anticline reservoir helped the operator determine if a zone, believed to be safely updip from the waterdrive in a mature low-resistivity oil- and gas-producing zone, would produce salt water or hydrocarbons. The CMR porosities and T_2 distributions have been added to the standard density neutron PLATFORM EXPRESS wellsite display *(next page)*.

Several sandstone intervals, Zones A, B and C, are easily identified by their longer T_2 distributions that may correspond to hydrocarbons isolated in water-wet rocks or large water-filled pores. Zone C is more conductive—indicating water, but the CMR total porosity reads less than the density-porosity—indicating gas. There are high-resistivity sands in Zones A and B that are difficult to interpret from raw logs alone. The picture is confusing.

A petrophysical analysis, combining CMR and PLATFORM EXPRESS data over this interval, reveals the nature of the reservoir complexities—lithologic changes and the presence of a waterdrive flood front *(page 50, top)*. This interpretation—including the CMR-derived permeability, verified by subsequent core analysis—along with irreducible water analysis, shows that the upper resistive sand, Zone A, is productive and contains oil with little free water. The middle, less resistive sand, Zone B, contains less oil with a significant amount of potential producible water. The low-resistivity sand, Zone C, appears to contain some oil, but with a large amount of free water most likely coming from the waterflood.

13. Whenever oil-base mud is used in water-wet rocks, it is easy to identify bound versus free fluid. Bound-fluid water has a short T_2, and oil-base mud flushing into the free-fluid pore space has a long T_2. The T_2 cutoff is obvious, making free fluid and bound fluid easy to distinguish for Timur-Coates permeability calculations.

The operator, hoping that the logs might have been affected by deep invasion, completed and tested the lower sand, Zone C. However, it produced only salt water, consistent with the petrophysical interpretation. After a plug was set above this zone, the upper sands were completed and produce 100 BOPD [16 m^3/d] with only a 10% water cut, which is also in agreement with the expectations from the ELAN interpretation. It is clear that combining the porosity discrimination and permeability information from CMR measurements with other logs, such as resistivity and nuclear porosity, helps explain what is happening to the waterdrive and hydrocarbons in pay zones in this common, but complex, reservoir.

Logging for Bound-Fluid

Bound-fluid logging, a special application of NMR porosity logging, is based on the ability of NMR to distinguish bound-fluid porosity from free- or mobile-fluid porosity. Bound-fluid porosity is difficult to measure by conventional logging methods. A full NMR measurement requires a long wait time to polarize all components of the formation, and a long acquisition time to measure the longest relaxation times. However, experience has shown that the T_2 relaxation time of the bound fluid is usually less than 33 msec in sandstone formations and less than 100 msec in carbonate formations. In fast bound-fluid NMR logging, it is possible to use short wait times by accepting less accuracy in measuring the longer T_2 components. In addition, a short echo spacing and an appropriate number of echoes reduce the acquisition time and ensure that the measurement volume does not change significantly because of the faster tool movement. This logging mode can acquire NMR data at speeds up to 3600 ft/hr [1100 m/hr] because of the short relaxation times of the bound fluid.

The bound fluid volume can be used in conjunction with other high speed logging measurements to calculate two key NMR answers—permeability and irreducible water saturation, S_{wirr}. Typically, the density log is used in shaly sands, and the density-neutron crossplot porosity log is used in gas sands, carbonates and complex lithologies. The epithermal neutron porosity from the

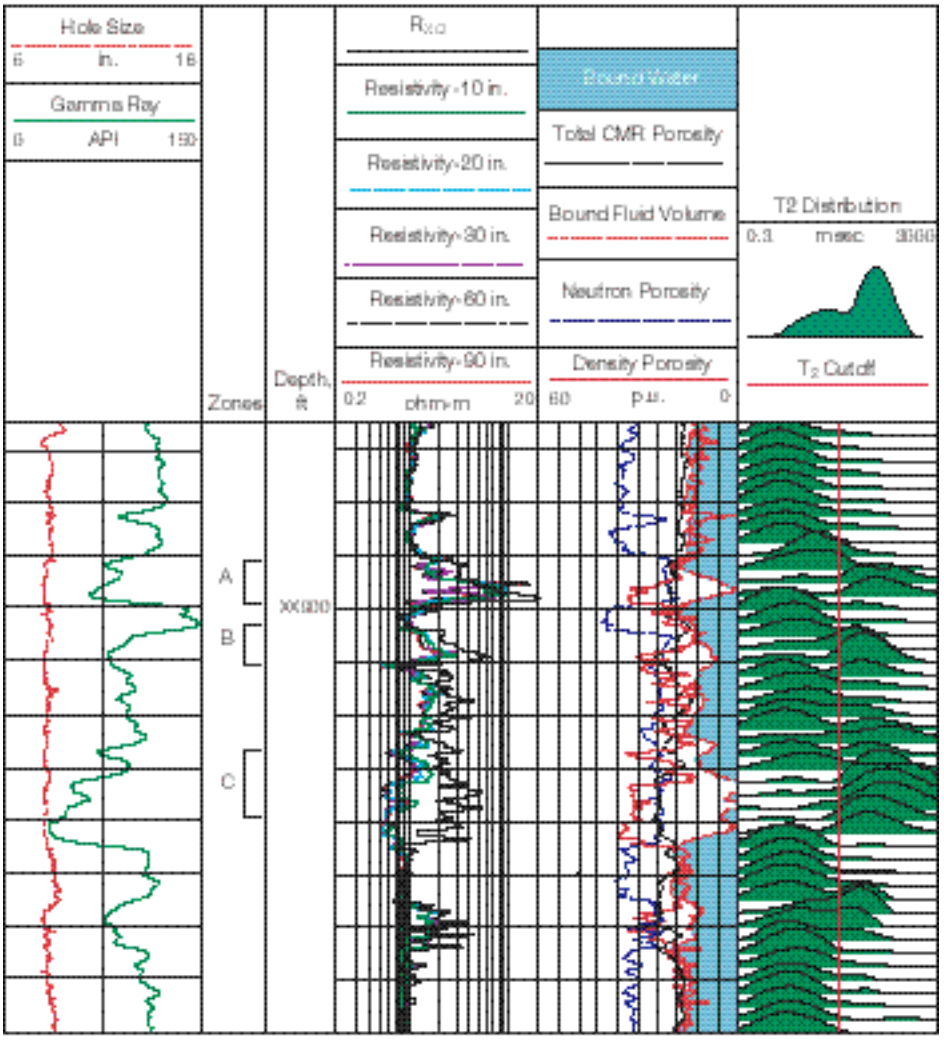

Wellsite PLATFORM EXPRESS display. This example shows long T_2 components in the low-resistivity pay sand, Zone C. This appears to the CMR tool to contain mostly free water in large pores, but could contain isolated hydrocarbons with long T_2. The upper two zones have high resistivity and potentially contain hydrocarbons. The total CMR porosity matches the density porosity except in the lower sections of Zones A and C, due to incomplete polarization (with a 1.3 sec wait time) of the hydrocarbons.

Solving the mystery with ELAN interpretation. High permeability derived from the CMR tool, track 2, with water saturation, track 3, and irreducible water analysis, track 4, show that the low-resistivity pay sand in Zone C will produce only water, probably from the flood drive. The upper sand, Zone A, contains oil with only a little free water. Zone C tested 100% salt water, whereas the upper zone is producing 100 BOPD with a low water cut. Note the excellent agreement between the CMR permeability and core-derived permeability (black circles) in track 2.

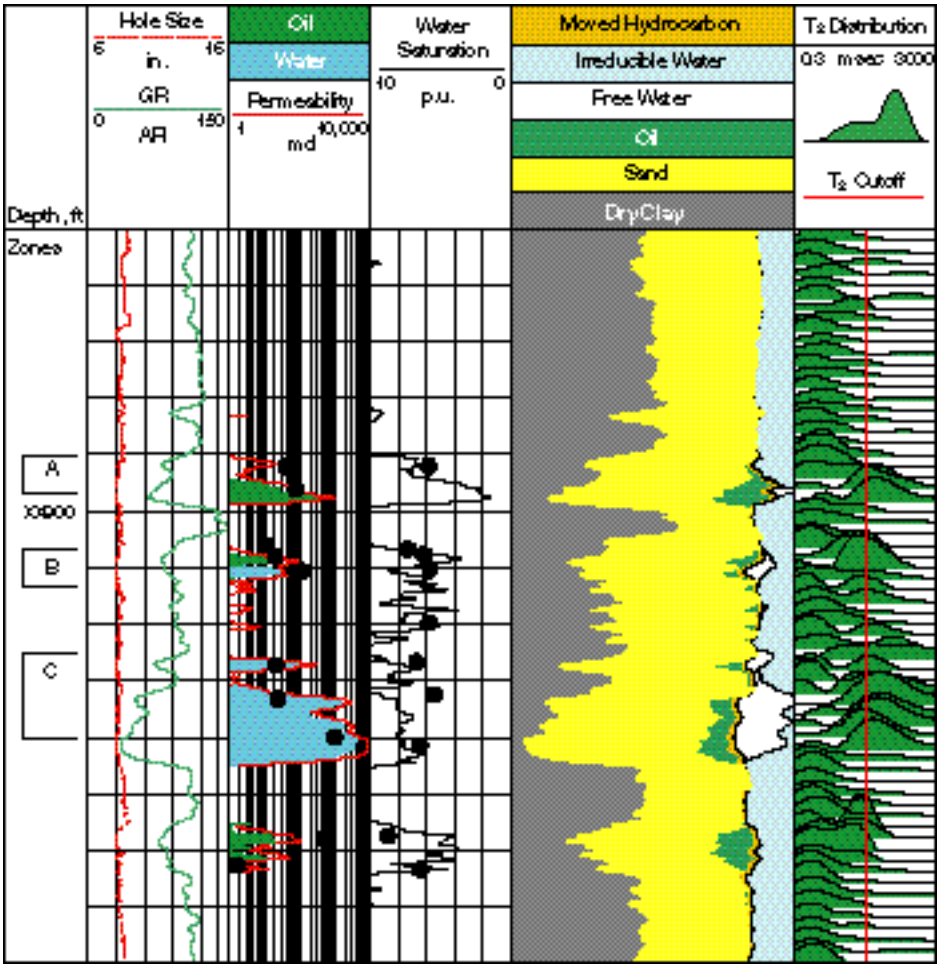

Bound-fluid logging with water-free production in a long oil-water transition zone. CMR readings indicate water-free production above XX690 ft, where the water volume, ϕS_w, computed from resistivity logs matches the bound-fluid volume (BFV) from the CMR tool. Even though bound-fluid logging speeds are fast, long T_2 components are seen in the CMR T_2 distributions.

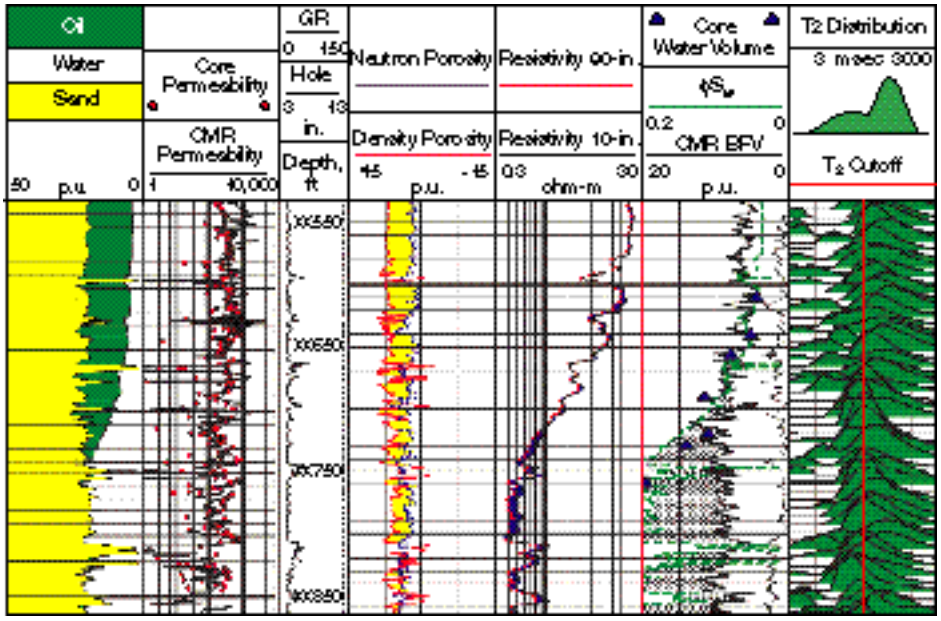

APT tool is especially accurate because it is immune to the thermal neutron absorber effects frequently found in shales.[14]

Bound-fluid logging can also be used to detect heavy oil, since many high-viscosity oils have T_2 components below the 33-msec or 100-msec cutoffs and above the 0.3-msec detection limit of the CMR-200 tool. These oils will be properly measured in a bound-fluid log.

Our first example of bound-fluid logging comes from the North Sea, where long transition zones and zones of low-resistivity pay often lead to uncertainty about the mobile fluid being oil or water, or both (*previous page, bottom*). One method of predicting mobile water is to compare the bound-fluid volume, BFV, seen by the CMR tool with ϕS_w—the volume of water computed from the resistivity measurement. If the total water from the ϕS_w calculation exceeds the BFV measurement, then the excess water will be free fluid and therefore producible.[15] In this example, the CMR bound-fluid tool was run with the standard triple combo—neutron and density for total porosity and an AIT Array Induction Imager Tool for saturation—at 1500 ft/hr [460 m/hr]. The fast-logging CMR tool was run with a short wait time of 0.4 sec and 600 echoes. This well was drilled with an oil-base mud, which created a large signal at long T_2 times due to invasion of oil filtrate. To fully capture these long T_2 components for a total CMR porosity measurement, wait times of 6 sec would have been required, at a correspondingly slower logging speed of 145 ft/hr [44 m/hr].

An interpretation based on density, neutron and resistivity logs yields the lithology and fluid content. The T_2 distributions show significant oil-filtrate signal seen at late times despite the short wait time. The lithology analysis shows little or no clay, consistent with the lack of T_2 data below 3 msec.

In this well, a 100-msec cutoff was used to differentiate the bound-fluid volume from the free fluids; this is verified by excellent agreement with core permeability using the default Timur-Coates equation. Ideally, the T_2 cutoff should be confirmed independently, for example by careful sampling with the MDT Modular Formation Dynamics Tester tool around the oil-water transition depths.

In another example, a real-time wellsite quicklook display was developed for combining CMR bound-fluid logging with the PLATFORM EXPRESS acquisition at 1800 ft/hr [550 m/hr] in the Gulf of Mexico. In offshore wells, with hourly operating expenses that far exceed logging costs, fast logging and immediate answers are critical for timely decision-making at the wellsite. The field quicklook incorporates the CMR measurements into a Dual-Water saturation computation. The results are total porosity from the neutron-density and water saturation from the AIT induction tools *(above)*. The wellsite permeability computation, track 2, uses the CMR bound-fluid results in a Timur-Coates analysis with two estimates of total porosity—one from the traditional neutron-density crossplot porosity, and the other from a density-derived porosity.[16]

The first porosity estimate is more accurate in the shaly sections but requires free- and bound-water resistivity and wet-clay porosity parameters and is limited by the vertical resolution of the neutron measurement. The second porosity estimate has the advantages of not requiring any parameter picks for the shaly intervals and also has the higher vertical resolution inherent in the density measurement. The field-derived results show both sand Zones, A and B, with good production potential and with low water cut. These logging results agree well with the sidewall core permeabilities and porosities measured later, shown as circles in tracks 2 and 4.

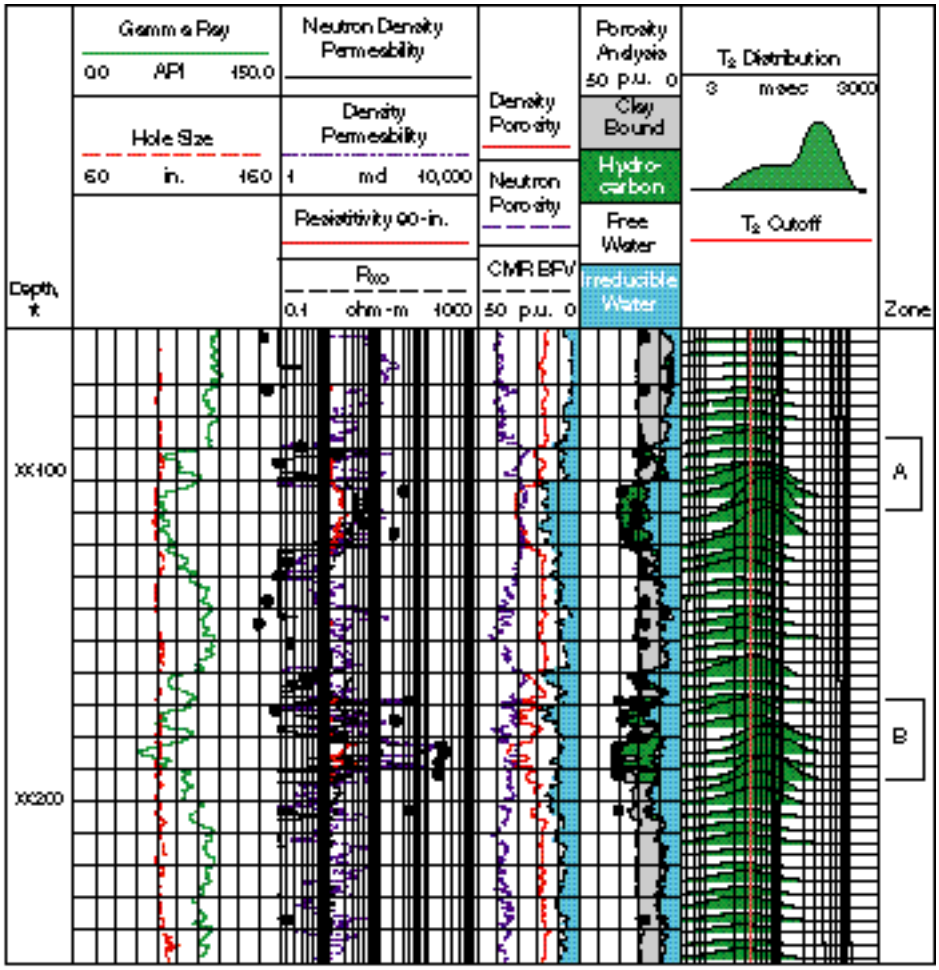

PLATFORM EXPRESS-CMR wellsite quicklook. The field interpretation results from high-speed CMR logging enable the operator to quickly identify that hydrocarbon pay Zones A and B, have high permeability, track 2, and high potential for water-free production because all the water in the interval, as shown in track 4, is either clay-bound or irreducible. The wellsite interpretation results also compared well with core analysis obtained later.

Repeatability of Fast BFV Logging—This example shows that accurate and repeatable bound-fluid volumes and permeabilities can

14. Scott HD, Thornton JL, Olesen J-R, Hertzog RC, McKeon DC, DasGupta T and Albertin IJ: "Response of a Multidetector Pulsed Neutron Porosity Tool," *Transactions of the SPWLA 35th Annual Logging Symposium*, Tulsa, Oklahoma, USA, June 19-22, 1994, paper J.
15. The BFV log measures the capillary-bound and non-mobile water.
16. LaVigne J, Herron M and Hertzog R: "Density-Neutron Interpretation in Shaly Sands," *Transactions of the SPWLA 35th Annual Logging Symposium*, Tulsa, Oklahoma, USA, June 19-22, 1994, paper EEE.

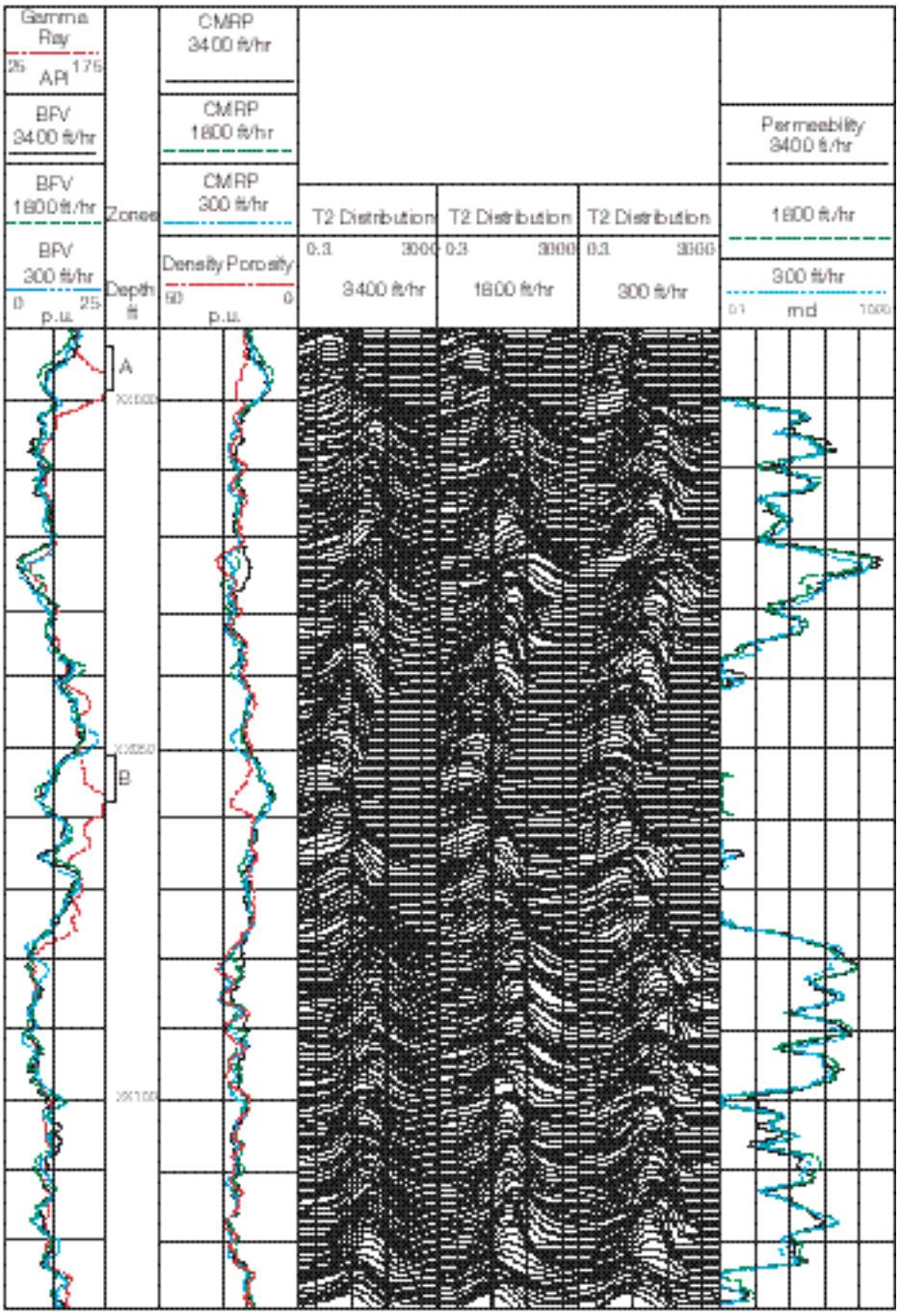

□*Repeatability of bound-fluid logging. Logs and T_2 distributions from three runs at 300, 1800 and 3400 ft/hr in the same well show how well the bound-fluid volumes, track 1, agree even at fast logging speeds. The permeability results, track 6, from CMR bound-fluid logging overlie even at the highest logging speeds. The T_2 distributions are similar, though the peaks in the sands seem to change somewhat, because there are not enough echoes in the fast logging measurement to completely characterize the slower relaxations. The longest T_2 components disappear in the fast-logging mode.*

be measured at high logging speeds *(above)*. Three runs were made through a series of sand-shale zones, where fresh water makes producibility evaluation difficult and high-precision bound-fluid determination is important. The three CMR passes were made with 0.2-sec wait time, 200 echoes at 3400 ft/hr [1040 m/hr]; 0.3 sec wait time, 600 echoes at 1800 ft/hr [549 m/hr]; and finally at 2.6 sec wait time, 1200 echoes at 300 ft/hr [92 m/hr]. The data were processed with total CMR porosity to give T_2 distributions from 0.3 msec to 3 sec, shown in tracks 3, 4 and 5 for each run. The three bound-fluid BFV logs, computed with default 33-msec T_2 cutoff and five-level stacking, are shown in track 1. They agree well with each other, having a root-mean-square error on the bound-fluid volumes about of 1.2 p.u., which is comparable to the typical statistical error found in other non-NMR porosity logs. The BFV curves correlate well with the gamma ray except in Zones A and B, with the shortest T_2 values, where the relaxation may be too rapid to be seen by the CMR tool.

Permeability estimates, in track 6, were based on the standard Timur-Coates equation. CMR bound-fluid logs and a robust total porosity estimator based on the minimum of the density and neutron-density porosities were used to compute the free-fluid and the bound-fluid volumes used in this permeability equation.[17] At these logging speeds, all three permeability estimates overlie one another, typically within a factor of 2.

Integrated Answers

Bound-fluid logging is one example of how CMR measurements combine with other logging measurements to provide a simple, more accurate picture of the formation in a fast, more efficient manner. The CMR tool can be combined with the MDT tool to give better producibility answers. The in-situ, dynamic MDT measurements complement the CMR continuous permeability log, and help verify the presence of producible hydrocarbons. Wellsite efficiency is substantially increased when MDT sampling depths are guided by CMR results.

Reservoirs often exhibit large vertical heterogeneity due to the variability of sedimentary deposition, such as in laminated formations. In vertical wells, formation properties can change over distances small compared to the intrinsic vertical resolution of logging tools. In horizontal wells, the drainhole can be located near a bed boundary with different formation properties above and below the logging tools. It is important that all logging sensors face the same formation volume.

Two logging measurements that investigate the same rock and fluid volume in a formation are said to be coherent. Conventional log interpretation methods can be limited by a lack of volumetric coherence between logs. For example, when subtracting the bound-fluid porosity response of an NMR tool from the total porosity response of a nuclear tool to compute a free-fluid index, care must be taken to ensure that the

17. Singer JM, Johnson L, Kleinberg RL and Flaum C: "Fast NMR Logging for Bound-Fluid and Permeability," *Transactions of the SPWLA 38th Annual Logging Symposium*, Houston, Texas, USA, June 15-18, 1997, paper PP.

nuclear tool does not sample a different volume than the NMR tool.[18]

An interesting example of combining CMR logging with other coherent measurements, is the method of determining formation silt volume developed with Agip.[19] Silt is an important textural component in clastic rocks because it relates to the dynamic conditions of transportation and deposition of sediments. The quality of a reservoir is determined by the amount of silt present in the rock formation. Fine silt drastically decreases permeability and the ability of a reservoir to produce hydrocarbons. The silt can be of any lithology; and, since it is related only to grain size, its volume and deposition properties can be determined with the help of CMR logging, in combination with EPT measurements.

Dielectric propagation time and attenuation increase with silt volume. These two logs, coupled with the APT epithermal neutron porosity, provide a porosity interpretation unaffected by the large thermal absorbers typically associated with silts and shales in formations, and are therefore appropriate in determining silt volume in complex lithologies.

Accuracy in determining silt volume, as well as a host of other parameters—permeability, fluid volumes and mobility—depends upon a high coherence between logging measurements.

The CMR measurement's ability to characterize grain size, using the T_2 distributions, coupled with other complimentary logs, was successfully used to understand a complex reservoir sequence of thinly laminated sands, silt and shales in the presence of water and gas *(right)*. The well was drilled with fresh water-base mud. The EPT dielectric attenuation and propagation time curves, showing high bed resolution in track 1, cross each other—clearly identifying the sequence of silty sands and shales. Perme-

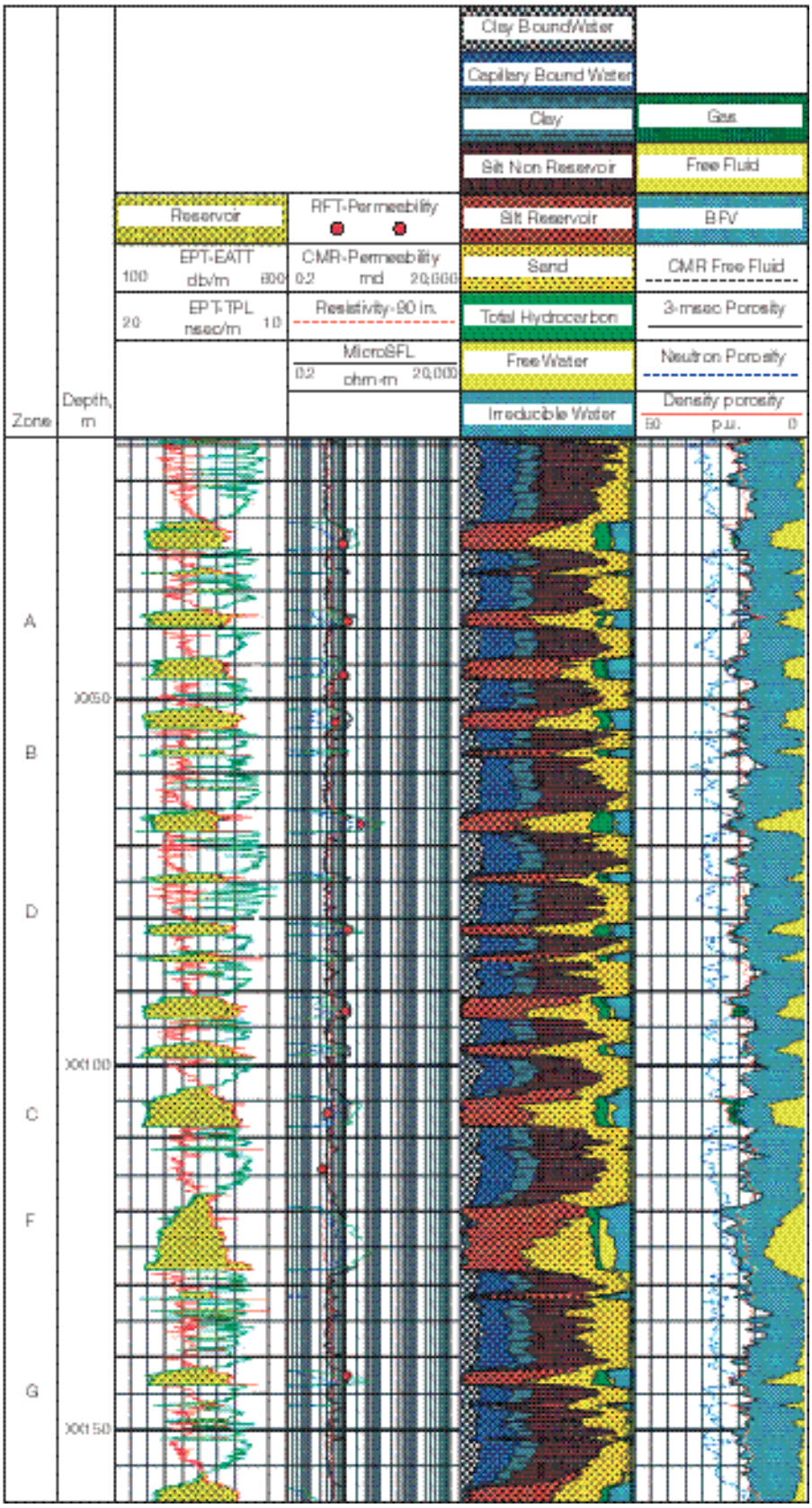

Avoiding water production in thinly layered gas sands with CMR data combined with other coherent logging measurements. There are nearly 20 gas pay-sands showing in this interval, all showing similar log profile characteristics—separation of the EPT dielectric propagation time TPL, and attenuation EATT, logs in track 1 and the free-fluid volumes from CMR and epithermal neutron porosity, in track 4. The interpretation results identify three Zones (A, C and the lower part of Zone F) that contain free water in the reservoirs. The CMR tool responds well to thin beds (Zones B, D and G).

18. An example of an incoherent result would be the case in which a nuclear tool is sampling a few inches of formation, and an NMR tool is sampling several feet of formation, or vice versa. Then the net free fluid could be distorted and incorrectly computed by large porosity changes within the sample volume caused by shale laminations in the formation. If the nuclear and NMR tools are sampling the same volume of rock, then the combined results will always be correct because the different measurements will be *volume matched*.

19. Gossenberg P, Galli G, Andreani M and Klopf W: "A New Petrophysical Interpretation Model for Clastic Rocks Based on NMR, Epithermal Neutron and Electromagnetic Logs," *Transactions of the SPWLA 37th Annual Logging Symposium*, New Orleans, Louisiana, USA, June 16-19, 1996, paper M.

Gossenberg P, Casu PA, Andreani M and Klopf W: "A Complete Fluid Analysis Method Using Nuclear Magnetic Resonance in Wells Drilled with Oil Based Mud," *Transactions of the Offshore Mediterranean Conference*, Milan, Italy, March 19-21, 1997, paper 993.

Gas-Corrected Porosity from Density-Porosity and CMR Measurements

In zones containing unflushed gas near the borehole, total CMR porosity log—TCMR—underestimates total porosity because of two effects: the low hydrogen concentration in the gas and insufficient polarization of the gas due to its long T_1 relaxation time. On the other hand, in the presence of gas, the density-derived porosity log DPHI, which is usually based on the fluid being water, overestimates the total porosity because the low density of the gas reduces the measured formation bulk density. Thus, gas zones with unflushed gas near the wellbore can be identified by the deficit or separation between DPHI and TCMR logs—the NMR gas signature. The method of identifying gas from the DPHI/TCMR deficit does not require that the gas phase be polarized.[1]

The advantages of this method of detecting gas include:

- faster logging in many environments since the gas does not have to be polarized[2]
- more robust gas evaluation since the deficit in porosity is often much greater than a direct gas signal
- total porosity corrected for gas effects.

As an aid to interpreting gas-sand formations, the gas-corrected porosity, $\varphi_{gas\text{-}corr}$, and gas bulk-volume, V_{gas}, equations are derived from a petrophysical model for the formation bulk density and total CMR porosity responses.

The mixing law for the density log response is:

$$\rho_b = \rho_{ma}(1-\phi) + \rho_f \phi (1-S_g) + \rho_g \phi S_g$$

and for the total CMR porosity response:

$$TCMR = \phi S_g (HI)_g f_g + \phi (1-S_g)(HI)_f .$$

In these equations, ρ_b is the log measured bulk-formation density, ρ_{ma} is the matrix density of the formation, ρ_f is the density of liquid phase in the flushed zone at reservoir conditions, ρ_g is the density of gas at reservoir conditions, and φ is the total formation porosity.

$(HI)_g$ is the hydrogen index—the volume fraction of fresh water that would contain the same amount of hydrogen—of gas at reservoir conditions, and $(HI)_f$ is the hydrogen index of fluid in the flushed zone at reservoir conditions. S_g is the flushed zone gas saturation.

$f_g = 1 - \exp\left(-\frac{W}{T_{1,g}}\right)$ accounts for the polarization of the gas, where W is wait time of the CMR tool pulse sequence, and $T_{1,g}$ is the longitudinal relaxation time of the gas at reservoir conditions.

To simplify the algebra, a new parameter, $\lambda = \frac{\rho_f - \rho_g}{\rho_{ma} - \rho_f}$, is introduced, and formation bulk density is eliminated by introducing density—derived porosity, $DPHI = \frac{\rho_{ma} - \rho_b}{\rho_{ma} - \rho_f}$.

Solving these equations for the gas-corrected porosity, $\varphi_{gas\text{-}corr}$, one gets:

$$\varphi_{gas\text{-}corr} = \frac{DPHI\left(1 - \frac{(HI)_g * P_g}{(HI)_f}\right) + \frac{\lambda * TCMR}{(HI)_f}}{\left[1 - \frac{(HI)_g * P_g}{(HI)_f}\right] + \lambda},$$

and for the volume of gas, one gets:

$$V_{gas} = \frac{DPHI - \frac{TCMR}{(HI)_f}}{\left[1 - \frac{(HI)_g * P_g}{(HI)_f}\right] + \lambda}.$$

The gas saturation can be obtained from these equations by simply dividing the latter by the former. Note that the gas-corrected porosity, $\varphi_{gas\text{-}corr}$, is the NMR analog of the neutron/density log crossplot porosity, and is always less than *DPHI* and greater than $TCMR/(HI)_f$.

—Bob Freedman

1. To be able to attribute this deficit to gas, the wait time for the logging sequence must be sufficiently long to polarize all the liquids, including formation water and mud filtrate.
2. Oilbase muds are the exception and require long wait times due to the long T_1 relaxation time of oil filtrate.

ability curves were computed from the CMR bound-fluid log using both the Timur-Coates equation and the Kenyon equation with the logarithmic mean of T_2.[20] Both give reasonable agreement with permeability results derived from core and the RFT Repeat Formation Tester tool.

The dry sand, silt and clay volume interpretation model, shown in track 3, includes clay-bound water, capillary-bound water (or irreducible water), and movable water *(next page, top)*. By subtracting the irreducible water measured directly by the CMR bound-fluid log from total volume of water, φS_w, computed from R_t after clay corrections, all free water zones within the reservoirs are clearly determined. For example, Zone F cannot be perforated without risk of large water production. Apart from Zones A and F, most of the other reservoirs show dry gas. The epithermal neutron and density porosity logs are shown along with NMR logs in track 4. There are intervals with clear examples of gas crossover between the density-neutron porosity curves. Also, the separation between the APT neutron porosity and CMR porosity provides a good estimate of clay-water volume.

The logs show excellent correlation between the EPT and CMR curves. The sequence of fining-up grain size in the sands through Zone F is displayed on the logs as an increasing silt index. This is confirmed by increasing attenuation and propagation times on the EPT logs—because of increasing conductivity in the silt, and an increase in bound-water porosity in the CMR logs—implying a decrease of movable fluid. The profile on other pay reservoirs between both tools shows similar characteristics, especially in the EPT curve separation and the free-fluid volumes from the CMR measurements.

The CMR measurements complement other coherent logging measurements, such as dielectric, Litho-Density, microresistivity, neutron capture cross sections and epithermal neutron porosity, in providing a critical evaluation and complete interpretation in these complex formation environments. The Litho-Density tool is needed for lithology—to determine the T_2 cutoff for CMR bound-fluid

20. Kenyon WE, Day PI, Straley C and Willemsen JF: "A Three-Part Study of NMR Longitudinal Relaxation Properties of Water-Saturated Sandstones," *SPE Formation Evaluation* 3 (1988): 622-636.
21. Freedman et al, 1997, reference 10.
22. Bass C and Lappin-Scott H: "The Bad Guys and the Good Guys in Petroleum Microbiology," *Oilfield Review* 9, no. 1 (Spring 1997): 17-25.

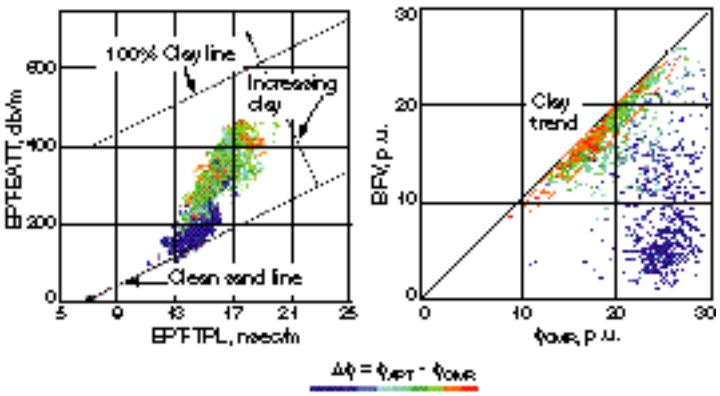

□Silt volume interpretation using EPT, APT and CMR logs. The data in the crossplots come from a mixture of sands, mica and feldspar. EPT attenuation, EATT, and propagation time, TPL, are crossplotted *(left)* **along with the difference between APT epithermal neutron porosity and CMR 3-msec effective porosity, shown as a Z-axis discriminator. There are two clusters of points. One is for the silty sand where gas is present** *(lower cluster)*. **There is a departure from the sandstone line when silt increases. The second cluster is in several nonpay reservoirs where clay minerals, associated with fine silt, form the shales. The APT-CMR effective porosity difference increases in proportion to the clay content due to the clay-bound water. Since the gas content is properly controlled on the EPT crossplot, the dielectric data are used to apply accurate gas corrections on the CMR porosity logs. On the CMR stand-alone crossplot** *(right)*, **the silt index increases with the bound-fluid values. The scatter in the CMR data is a gas effect induced by low polarization and variation in hydrogen index. The APT-CMR difference porosity is used again for Z-axis discrimination and the two clusters are identified. Fine silt in the shales follows the 45° clay trend line downwards to the clay endpoint at the origin. Except for the gas scatter on CMR porosity, the crossplot confirms the high coherence existing between the three logs.**

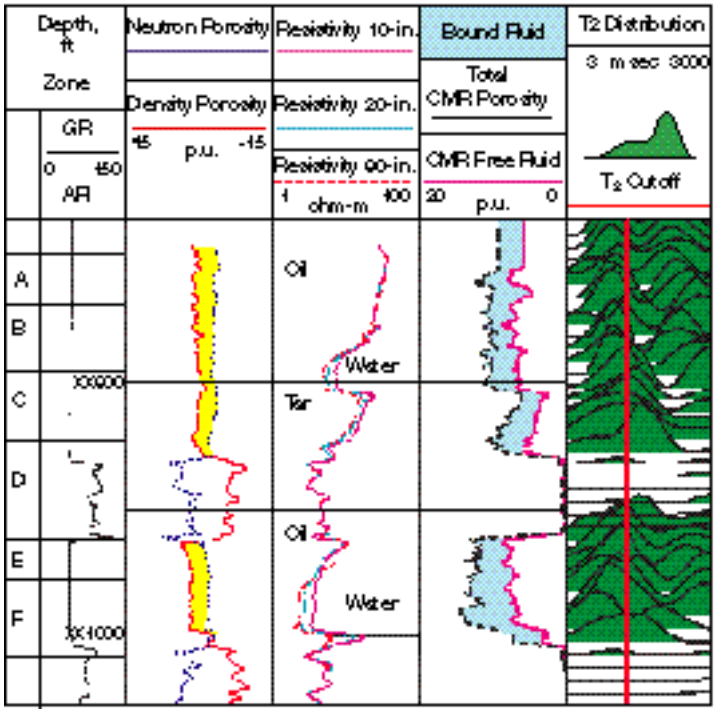

□Tar zones detected by the CMR tool. In water, gas or oil, the CMR tool has a clear tar signature as seen in Zone C—a suppression of the long T_2 components (track 5) and a reduced total porosity (track 4). In this well the CMR tool is able to confirm—by the presence of large T_2 contributions from oil and no reduction in total CMR porosity—that the lower oil zone (Zone E) is not tar, but mobile oil, which could be trapped by a local stratigraphic closure.

logging—and the salinity independent CMR water volume is used to correct the dielectric and resistivity logs—used for fluid saturation.

Identification of Oil Viscosity and Tar Deposits—A trend to produce heavy-oil from shallow reservoirs is creating the need to detect high viscosity oil and tar deposits. Frequently, due to the shallow depths and the complex filling history of the structures, reservoirs were charged, then later breached and recharged. This results in significant changes in the properties of the hydrocarbons throughout the reservoir sections. One way to distinguish and identify these oils is to measure their viscosity in situ using bulk relaxation times from the CMR data. The bulk relaxation rates of different oils can be measured with reasonable accuracy, between 2 and 10,000 cp, using the CMR tool.[21]

Field examples show that CMR log-derived viscosities match drillstem test-derived values. It is important to determine which part of the T_2 signal distribution is from the oil bulk relaxation decay. In clean, coarse sands containing high-viscosity oil, this is a straightforward process, because the oil, having a fast decay, is isolated from the water-wet rock having a slower decay, and surface relaxation has little effect on the fast bulk oil decay. For low-viscosity oils in fine-grained rocks, the bulk oil relaxation rates are much slower and can easily be separated from the water-saturated rock signal.

In some settings, over geological time, oils have come into contact with water-borne bacteria that produce impermeable seals—tar deposits at oil-water contacts.[22] These reservoirs may receive a further oil charge, which encases a tarry zone inside the hydrocarbon zone. In such a position, the tar zone could have a dramatic effect on the management of the field during production.

The tar, surrounded by other hydrocarbons, appears similar to the surrounding fluids when logged with non-NMR techniques. Even when cored intervals are available, the tar may be overlooked if the core samples are cleaned, as they traditionally are, before analysis. However, the CMR signature in a tar zone is quite clear and distinct from that of more mobile hydrocarbons or water. It has been suggested that long hydrocarbon chains within the tar cause it to behave almost like a solid—dramatically shortening the T_2 response. Tar is detected by the reduction in NMR porosity.

An example from the North Sea shows the clear tar detection signature—missing porosity and short T_2 decays *(left)*. The well was drilled with an oil-base mud through several oil and water zones identified in track 2.

When the tar is in a conductive water zone, as it is in this example, it can be easily identified by resistivity measurements. However, tar is frequently located in hydrocarbon zones, where there is no resistivity contrast between tar and nontar hydrocarbon intervals. In such cases, NMR is the only routine logging measurement that can identify the tar.

Like tar, heavy oil has a short T_2 relaxation decay time, so detecting heavy oil is similar to detecting tar, except that the heavy-oil relaxation times are sufficiently long to be captured by the total porosity response of the CMR-200 tool. Essentially, the heavy-oil T_2 contribution shifts the signal below the 3-msec T_2 cutoff, but not below the 0.3-msec detection limit of the CMR-200 tool (*right*).

This example is from a heavy-oil reservoir in California. The low-gravity (12 to 16°API) oil is produced by a steam-soak injection method. The logs show that all porosity logs—total porosity, 3-msec effective porosity, density and neutron porosity—agree in the lower wet Zone B. The CMR porosities agree in the wet zone because the formation does not have T_2 values below 3-msec associated with clay-bound porosity or microporosity. In the upper oil-bearing Zone A, total CMR-porosity reads about 5 p.u. higher than the 3-msec porosity over most of this interval, because the heavy oil has considerable fast relaxing components below the 3-msec T_2 sensitivity limit of the early 3-msec porosity measurement. The different responses of the two CMR porosity measurements to the heavy oil provide a clear delineation of the oil zone and show the oil-water contact between Zones A and B.

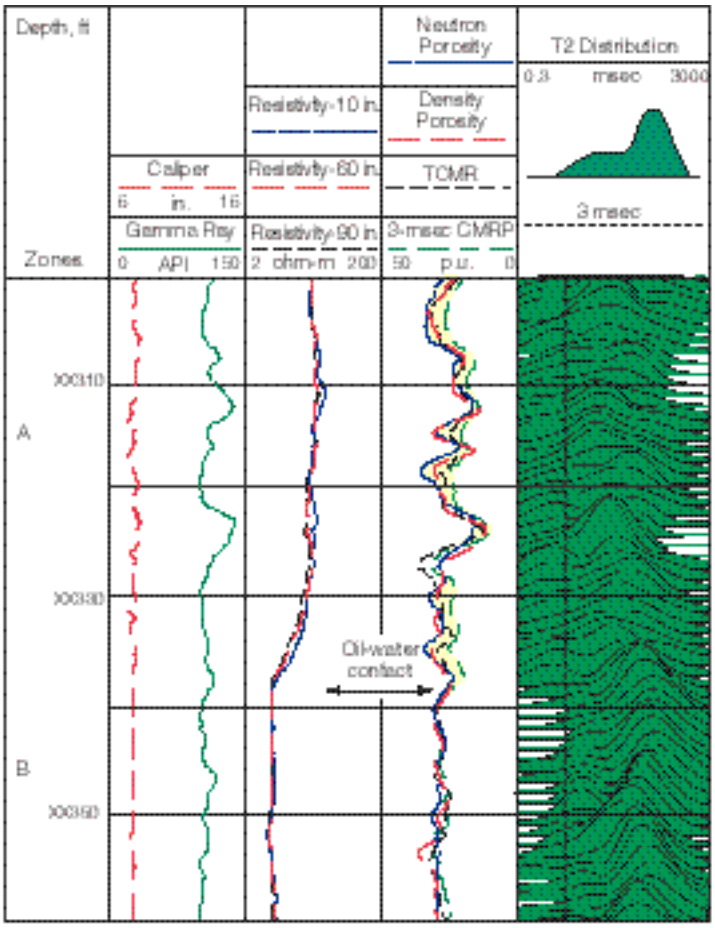

□*How to see a heavy-oil water contact with total CMR porosity. The oil-bearing Zone A and the oil-water contact between Zones A and B are clearly delineated by the separation between the total CMR porosity log, TCMR, and the 3-msec porosity log, CMRP, shown in track 3. The oil-water contact is confirmed by the resistivity logs in track 2. The large heavy oil contribution to the total porosity can be seen by short relaxation decay components above the oil-water contact in the T_2 distribution in track 4.*

Logging Saves Dollars—Combining geochemical logs with CMR-derived permeability and free-fluid data, a major oil company was able to select only productive zones for stimulation—saving $150,000 in a South Texas well.[23] The objective was to complete, including fracture simulation, three high-resistivity potential pay zones at the bottom of the well. Total porosity from CMR is approximately 10 to 15 p.u. in all zones, where free fluid varies from 1 to 10 p.u.

However, spectral data from the ECS Elemental Capture Spectrometer sonde indicate significant differences in clay and carbonate cement volumes between zones *(next page)*.[24] The two Zones, A and C, exhibit lower clay and higher carbonate—calcite cement—content than Zone B. Resistivity measurements and CMR-derived bound fluid and permeability correlate with the lithology changes. Increased clay volumes in Zone B represent shales that are clay-rich—suggesting a lower depositional rate.

These important lithological differences have significant influence on the electrical, mechanical and fluid flow properties of the reservoir intervals. Bound fluid and free fluids, measured by the CMR tool, vary widely for any given porosity, and have a large impact on the permeability.

Based on the logging results, Zone C was perforated and fracture stimulated and is currently producing gas at a rate of 6 MMcf/D with a very low water cut of 10 BWPD. The pessimistic estimates of free fluid volumes and permeability from the

23. Horkowitz JP and Cannon DE: "Complex Reservoir Evaluation in Open and Cased Wells," *Transactions of the SPWLA 38th Annual Logging Symposium*, Houston, Texas, USA, June 15-18, 1997, paper W.

24. Herron SL and Herron MM: "Quantitative Lithology: An Application for Open- and Cased-Hole Spectroscopy," *Transactions of the SPWLA 37th Annual Logging Symposium*, New Orleans, Louisiana, USA, June 16-19, 1996, paper E.

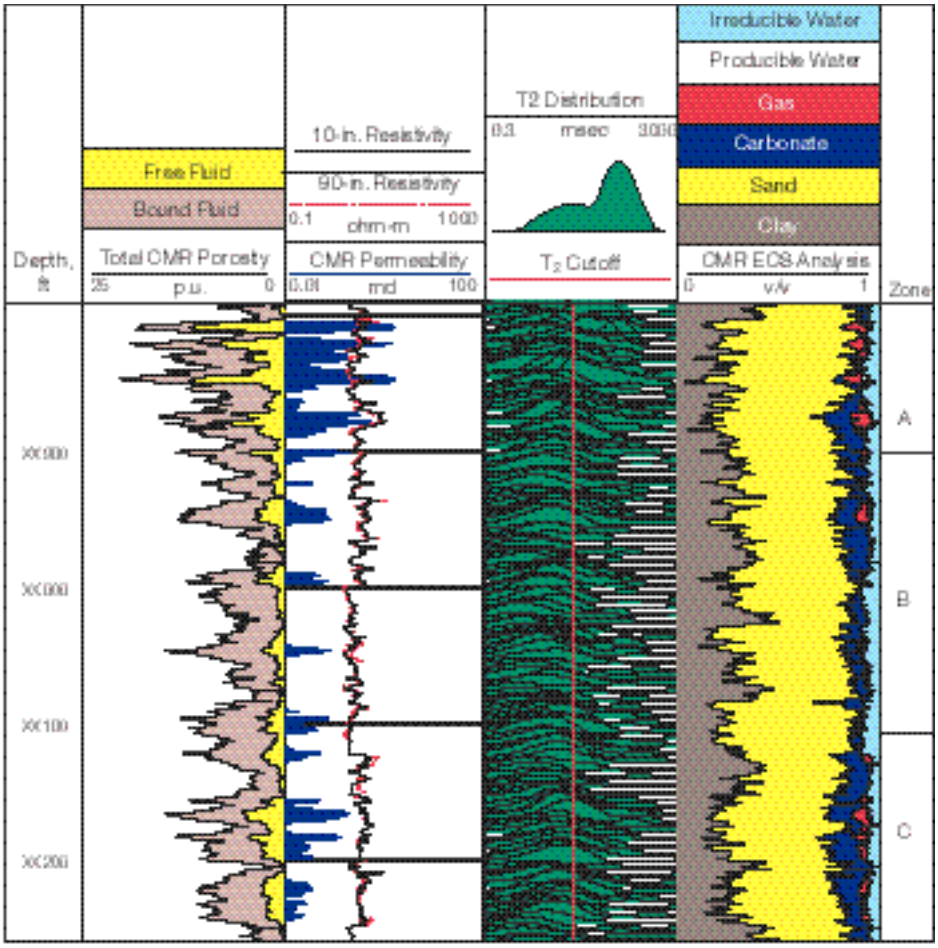

☐*CMR combined with geochemical logs from the ECS tool. Decreased free fluid (track 1) and permeabilities from CMR logs (track 2) and hydrocarbons from an ELAN interpretation (track 4) show the middle interval (Zone B) was not worth the expensive fracture job planned by the operator. The low permeability is due to clay and carbonates seen in this interval (track 4). Two other Zones (A and C) in the same well, were identified with lower clay, as seen by the geochemical logs, and CMR permeabilities are ten times better in these intervals. Zone C was completed and is producing gas at a rate of 6 MMcf/D and Zone A is expected to produce in excess of 10 MMcf/D.*

CMR tool, confirmed by the increased clay content shown by the geochemical logs, convinced the client to cancel the expensive fracture stimulation and abandon the large middle zone, Zone B. The upper zone, Zone A, is currently being perforated and a fracture stimulation is planned based on the CMR and ELAN interpretation results, with an expected gas production rate in excess of 10 MMcf/D.

The Outlook for the Future

This is an exciting time for petrophysicists, reservoir engineers and geologists who use well logging measurements. Recent improvements in NMR logging tool technology have dramatically increased the range of relaxation rates that can be measured in the borehole. Today, we can finally use these tools to differentiate bound and free fluids in the formation, determine permeability, and log faster for bound fluids. We have seen many examples of how to use these measurements to improve our understanding of complex shaly sand formations. The CMR and MRIL tools are commercial and their use is already routine in many parts of the world. However, there is much more to learn.

More work needs to be done to understand how to use T_2 distributions effectively in carbonate formations, with their extremely wide variations in porosity scale and structure. Our interpretation of NMR responses in shaly sand reveals bound and free fluids. In the future, we must extend the interpretation so that the measured relaxation decay times and the T_2 distributions in carbonates also reflect the mobility and dynamics of reservoir fluids in these far more complex pore structures.

—RCH